Systems & Control Letters 195 (2025) 105970

Contents lists available at ScienceDirect

Systems & Control Letters

journal homepage: www.elsevier.com/locate/sysconle

A dynamic event-triggered approach for observer-based formation control of multi-agent systems with designable inter-event time

Zeyuan Wang [a,*], Mohammed Chadli [a,*], Steven X. Ding [b]

[a] University Paris-Saclay Evry, 40 Rue du Pelvoux, Evry, 91020, France
[b] University of Duisburg–Essen, Bismarkstrasse 81 BB, Duisburg, 47057, Germany

ARTICLE INFO

Keywords:
Dynamic event-triggered control
Multi-agent systems
Formation control
Observer-based control
Distributed control
Designable inter-event time

ABSTRACT

This paper addresses the leader-following formation control problems for generic linear multi-agent systems under directed topology with designable inter-event time. A synthesis approach combining controller and observer design is developed under a dynamic event-triggered communication and control scheme. The proposed feedback control, state estimation, and event-triggered rules are distributed, and only local information is required for each agent to implement these algorithms. The proposed dynamic event-triggered protocol incorporates model-based estimation and clock-like auxiliary dynamic variables to prolong the inter-event time and economize the network resources. Furthermore, the inter-event time is designable, which allows more flexible tuning of communication frequency with only minor performance degradation. Sufficient conditions for formation control are established by linear matrix inequalities. The proposed method exhibits significant improvement over the dynamic event-triggered control methods described in the existing literature. Compared to the existing static event-triggered strategy, the proposed approach significantly reduces the utilization of communication resources while preserving asymptotic convergence to the desired formation. Comparative simulations demonstrate the validity and effectiveness of the proposed theoretical results.

1. Introduction

The study of multi-agent systems (MASs) originated in the 1980s and experienced rapid development in the mid-1990s. Advancements in technology, such as unmanned aerial vehicle coordination, underwater cooperation, and robot formation control, have highlighted the significance of cooperative control issues in multi-agent systems research. As the core of cooperative control, consensus issues have been widely studied in [1–3] and applied in engineering practice in recent years. One of the particularly intriguing topics is formation control, where a group of agents needs to achieve a desired geometric pattern to accomplish a cooperative mission. In the past few years, formation control has been extensively studied for both linear and nonlinear MASs and for MASs comprising homogeneous or heterogeneous agents under different scenarios. It can be based on leader-following consensus techniques [4] or leaderless consensus methods [5], depending on whether there is a reference model to be followed. A more detailed survey of formation control can be found in [6].

Communication and sampling play crucial roles in MASs. In time-triggered control systems, control updates and data transmissions occur periodically. This approach imposes a significant burden on communication networks and increases the demand for computing resources [7] for MASs, which leads to another communication issue under limited network bandwidth [8]. In order to address this issue, the event-triggered mechanism (ETM) emerges as a viable solution, which enables a minimum rate of data sampling, communication, and control update while still ensuring the consensus. The concept of ETM for stabilization control was first introduced in [9], then gained significant development and is applied in different dynamic systems. In [10], ETMs are used to handle the consensus problem of first-order linear MASs. It has been developed for generic linear MASs [11], nonlinear MASs [12], and heterogeneous MASs [13], with different constraints. In recent years, some studies have proposed fully distributed event-triggered control, where the control law and the event-triggering rule are independent of global information. For example, the control strategies described in [3,14] are fully distributed, whereas the ones in [1,15] are distributed only. In this paper, the proposed strategy is distributed since it requires graph Laplacian during the parameter design phase. A more comprehensive survey of ETMs for MASs can be found in [16].

* Corresponding authors.
E-mail addresses: zeyuan.wang@universite-paris-saclay.fr (Z. Wang), mohammed.chadli@universite-paris-saclay.fr (M. Chadli), steven.ding@uni-due.de (S.X. Ding).

https://doi.org/10.1016/j.sysconle.2024.105970
Received 10 February 2024; Received in revised form 11 July 2024; Accepted 12 November 2024

In recent years, based on the theoretical results of ETM, the dynamic event-triggered mechanism (DETM) was proposed in [17] to further prolong the minimum inter-event time (MIET). By introducing auxiliary dynamic variables (ADVs), the additional dynamic enables a lower sampling rate while still maintaining the control accuracy [18]. The DETM has been successfully applied in MASs in many different scenarios, including the leader-following formation control in [19]. In the context of a complex network environment, the paper in [20] introduces a DETM designed to handle both reliable and unreliable communication scenarios, taking into account the uncertainties associated with denial-of-service attacks. The study in [21] proposes a moving average approach for enhancing the stability of DETM. Additionally, in [22], a robust adaptive DETM is proposed to address challenges related to actuator faults and external disturbance. Despite the advantages of DETM, adjusting the minimum inter-event time (MIET) introduces challenges. The tuning methods often involve multiple design parameters and complex relationships between MIET and system parameters [23,24], posing practical difficulties in implementation. In [25,26], ADVs are designed as clock-like variables, providing more flexibility in selecting a preferred MIET. The tuning method involves only the upper bound of the ADV, represented as a scalar. By increasing this parameter, one can extend the MIET while still guaranteeing the consensus. However, it is important to note that longer MIET might sacrifice some convergence performance, and the transient behavior could be worse. Typically, the compromise of transient performance loss is deemed acceptable. The idea of [25] is also well-implemented in [27] for single nonlinear systems without consideration of state observer. In the work presented by [28], the designable MIET is achieved using the parametric Lyapunov equation. This approach is not limited to event-triggered control but extends to self-triggered control as well, with the Zeno behavior proven to be excluded. Additionally, in the work by [29], the designable MIET is realized through the proposed DETM along with considerations for input saturation.

Most above-mentioned ETM or DETM assume that the states of agents are all measurable, such as in [22,25–29]. However, this assumption is still far from reality since the internal state is not always available in application. One of the solutions is to implement state observers to estimate internal states based on inputs and outputs. Unlike the observer design for a single system, observers for MASs entail a co-design problem that involves event-triggered control and estimation. Some studies have addressed this issue. Indeed, in [30], the controller/observer co-design problem for generic linear MASs to handle leaderless consensus is studied. The results are further developed in [31] for the leader-following problem but only apply to second-order linear MASs. In [32], an observer-based ETM is proposed to deal with formation control problems under switching and directed topology. A more generic approach is proposed in [33], which uses linear matrix inequalities ($\mathcal{LMI}$s) to synthesize the controller and observer, but the final strategy is not distributed. The aforementioned studies are based on static event-triggered control, while few utilizes DETMs. Notably, the studies in [14,34] design observers-based DETM control while also eliminating the Zeno behavior. However, the complexity of parameter tuning presents a challenge in designing the MIET. Based on the above discussion, the synthesis of a distributed controller and observer under DETM with adjustable MIET has yet to be fully explored.

This work is inspired by [25–27], where DETMs are based on clock-like ADVs to facilitate the MIET adjustment. However, according to [26], a discontinuous Lyapunov function chosen could fail to achieve leader-following consensus. The resulting DETM only guarantees stability between two consecutive events but not globally. Based on the above discussion, a new Lyapunov function is proposed with a controller/observer synthesis method using the $\mathcal{LMI}$ approach for leader-following formation control problems, which is developed under a directed communication topology.

The main contributions of this paper are summarized as follows.

1. A distributed DETM for leader-following formation problems is proposed based on clock-like auxiliary variables, which significantly reduces the frequency of information exchange and communication updates while ensuring asymptotic convergence of the system. This mechanism allows the dynamical adjustment of the minimum inter-event time, which is crucial for adapting to varying network conditions and is not comprehensively addressed in the existing studies. Compared to the existing research [14,26,27,30,31,34], the proposed method provides heightened flexibility in tuning the MIET within directed networks. This capability allows for the limitation of communication frequency strictly below a preferred threshold. Supplementary performance analysis shows only limited performance change.
2. In contrast to previous studies, including [22,25–29], where the agent's states are assumed to be directly measured, the controller proposed in this paper relies on estimated state obtained through an observer. This introduces a co-design problem. The proposed observer-based DETM is notably closer to practical engineering applications.
3. Compared to [33], the observer-based controller and event-triggered rule designed for each agent are distributed and require only local information for implementation. Moreover, compared to [33,35,36], the proposed feedback control law adopts model-based combinatory measurement error, which grows slower than the trivial model-free measurement, enabling a longer inter-event time.
4. The directed communication topology used in this paper is closer to the practical settings. Sufficient conditions for determining the gain of the controller and observer under the proposed DETM are established using bilinear matrix inequalities ($\mathcal{BMI}$s), and the linearization approach with $\mathcal{LMI}$s is offered, which can be easily solved using numerical tools.

The rest of the paper is structured as follows: Section 2 provides basic graph theory. Section 3 presents the problem formulation and assumptions. The distributed DETM for formation control is detailed in Section 4. The effectiveness of the proposed strategies through numerical simulations as well as the quadratic performance analysis are demonstrated in Section 5. We conclude with a summary in Section 6.

Notations: Given a matrix $\boldsymbol{P}$, $\boldsymbol{P}^T$ denotes its transpose. If $\boldsymbol{P}$ is a square matrix, $\lambda_{\min}(\boldsymbol{P})$ and $\lambda_{\max}(\boldsymbol{P})$ denote the minimum and maximum eigenvalues of $\boldsymbol{P}$ respectively, and $\boldsymbol{P}^{-1}$ (resp. $\boldsymbol{P}^{-T}$) represents its inverse (resp. the transpose of the inverse). For a symmetric matrix $\boldsymbol{P}$, $\boldsymbol{P} < 0 (\leq 0)$ denotes that $\boldsymbol{P}$ is negative definite (negative semi-definite), and $\boldsymbol{P} > 0 (\geq 0)$ means $-\boldsymbol{P} < 0 (\leq 0)$. $\boldsymbol{I}_{m\times n}$ (resp. $\boldsymbol{I}_n$) denotes an identity matrix of dimension $m \times n$ (resp. of n). $\boldsymbol{0}_{m\times n}$ (resp. $\boldsymbol{0}_n$) denotes a zero matrix of dimension $m\times n$ (resp. of n). $\otimes$ denotes the Kronecker product. $\|\cdot\|$ denotes ℓ_2-norm for vectors or spectrum norm for matrices. Define $\mathrm{Sym}(\boldsymbol{P}) = \boldsymbol{P} + \boldsymbol{P}^T$. Let $*$ denote the symmetric entries in a matrix. Let $\mathbb{R}$ and $\mathbb{N}^+$ denote the set of real numbers and the set of positive natural numbers, respectively. For clarity of notation, matrices or vectors are represented using bold characters, while scalars are represented using non-bold characters.

2. Preliminaries

The communication topology of N ($N \in \mathbb{N}^+$) follower agents is represented by a directed graph $\mathcal{G} = (\mathcal{V}, \mathcal{E})$ consisting of a vertex set $\mathcal{V} = \{v_1, \ldots, v_N\}$ and an edge set $\mathcal{E} \subseteq \mathcal{V} \times \mathcal{V}$. Follower agent i and the leader are represented as vertices v_i and v_0, respectively. The adjacency matrix $\mathcal{A} = (a_{ij}) \in \mathbb{R}^{N\times N}$ of $\mathcal{G}$ is defined such that $a_{ii} = 0$, $a_{ij} = 1$ if v_i is connected to v_j (i.e., there exists a directed edge (v_i, v_j) from v_j to v_i) and $a_{ij} = 0$ otherwise. The Laplacian matrix $\boldsymbol{\mathcal{L}} = (l_{ij}) \in \mathbb{R}^{N\times N}$ is defined as $l_{ii} = \sum_{i\neq j} a_{ij}$ and $l_{ij} = -a_{ij}, i \neq j$. A neighbor j of agent i is defined as the agent j such that $a_{ij} = 1$. Denote $\mathcal{N}_i$ the set of neighbors of agent

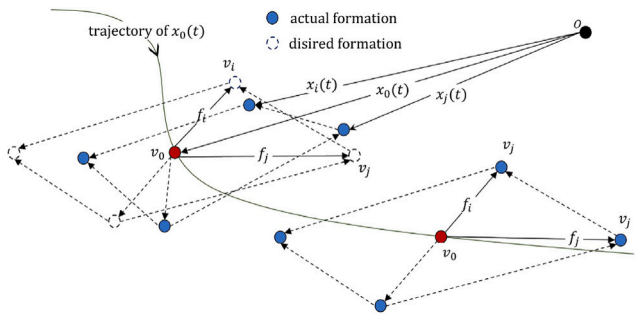

Fig. 1. Leader-following state formations, where red dots denote the leader, blue dots denote follower agents, O is the reference point, solid lines denote state vectors, and dashed lines denote information exchange. (For interpretation of the references to color in this figure legend, the reader is referred to the web version of this article.)

i. Define $\bar{\mathcal{G}} = (\bar{\mathcal{V}}, \bar{\mathcal{E}})$ the augmented graph of $\mathcal{G}$, with $\bar{\mathcal{V}} = \mathcal{V} \cup \{v_0\}$ and $(v_i, v_0) \in \bar{\mathcal{E}}$ if agent i is connected to the leader. Define leader adjacency matrix $\boldsymbol{\mathcal{D}} = \text{diag}(d_1, \dots, d_N)$ as a diagonal matrix where its diagonal element $d_i = 1$ if $(v_i, v_0) \in \bar{\mathcal{E}}$ otherwise $d_i = 0$. Define $\boldsymbol{\mathcal{H}} = \boldsymbol{\mathcal{L}} + \boldsymbol{\mathcal{D}}$. Given an agent node v_i, if for any $j \in \{1, \dots, N\} \backslash \{i\}$, there exists a directed path from v_i to v_j, then there exists a spanning tree whose root is the node v_i (which could also be the leader v_0).

3. Problem statement

Consider a linear MAS with N ($N \in \mathbb{N}^+$) follower agents and one leader represented by

$$\begin{cases} \dot{\boldsymbol{x}}_i(t) = \boldsymbol{A}\boldsymbol{x}_i(t) + \boldsymbol{B}\boldsymbol{u}_i(t), \quad i = 1, \dots, N \\ \boldsymbol{y}_i(t) = \boldsymbol{C}\boldsymbol{x}_i(t), \quad i = 1, \dots, N \\ \dot{\boldsymbol{x}}_0(t) = \boldsymbol{A}\boldsymbol{x}_0(t) \end{cases} \tag{1}$$

where $\boldsymbol{x}_i(t), i = 1, \dots, N$ and $\boldsymbol{x}_0(t)$ denote the states of follower agents and the leader, respectively. $\boldsymbol{y}_i(t)$ is the output of agent i, $\boldsymbol{u}_i(t) \in \mathbb{R}^m$ is the control input of agent i. $\boldsymbol{A} \in \mathbb{R}^{n\times n}$, $\boldsymbol{B} \in \mathbb{R}^{n\times m}$, $\boldsymbol{C} \in \mathbb{R}^{r\times n}$. Define time-invariant formation variables of follower agents as $\boldsymbol{f}_i \in \mathbb{R}^n$ and $\boldsymbol{f} = [\boldsymbol{f}_1^T, \dots, \boldsymbol{f}_N^T]^T$. Define the formation error of agent i as $\boldsymbol{\delta}_i(t) = (\boldsymbol{x}_i(t) - \boldsymbol{f}_i) - \boldsymbol{x}_0(t)$ and $\boldsymbol{\delta}(t) = [\boldsymbol{\delta}_1^T(t), \dots, \boldsymbol{\delta}_N^T(t)]^T$. The objective of this study is to design an event-based control law such that all follower agents and the leader achieve the desired formation, i.e.,

$$\lim_{t\to\infty} \|\boldsymbol{\delta}_i(t)\| = 0, \forall i \in \{1, \dots, N\} \tag{2}$$

Fig. 1 illustrates an example of formation, where four follower agents are supposed to form a parallelogram around the leader. $\boldsymbol{x}_i, \boldsymbol{x}_j$ are agents' states relative to the fixed reference point O, and the formation variable $\boldsymbol{f}_i$ is defined in a moving coordinate system where the leader is the reference point. In a special case of $\boldsymbol{f}_i = \boldsymbol{0}, \forall i = 1, \dots, N$, the leader-following formation becomes leader-following state consensus.

In order to estimate the agents' internal states, Luenberger-type observers are designed for each follower agent i and the leader to reconstruct the state $\boldsymbol{x}_i(t)$ and $\boldsymbol{x}_0(t)$:

$$\begin{cases} \dot{\tilde{\boldsymbol{x}}}_i(t) = \boldsymbol{A}\tilde{\boldsymbol{x}}_i(t) + \boldsymbol{B}\boldsymbol{u}_i(t) + \boldsymbol{L}_o(\tilde{\boldsymbol{y}}_i(t) - \boldsymbol{y}_i(t)) \\ \tilde{\boldsymbol{y}}_i(t) = \boldsymbol{C}\tilde{\boldsymbol{x}}_i(t) \end{cases} \tag{3}$$

where $\boldsymbol{L}_o \in \mathbb{R}^{n\times r}$ is the observer gain to be designed, and $\tilde{\boldsymbol{x}}_i(t)$ is the observer state. For the leader, the input $\boldsymbol{u}_0(t)$ is regarded as $\boldsymbol{0}$. Define observer error of agent i as $\boldsymbol{\zeta}_i(t) = \tilde{\boldsymbol{x}}_i(t) - \boldsymbol{x}_i(t)$ and $\boldsymbol{\zeta}(t) = [\boldsymbol{\zeta}_1^T(t), \dots, \boldsymbol{\zeta}_N^T(t)]^T$.

The proposed event-triggered control input $\boldsymbol{u}_i(t)$ of follower agent i is defined as

$$\begin{cases} \boldsymbol{u}_i(t) = \boldsymbol{K}\boldsymbol{z}_i(t) + \boldsymbol{K}'\boldsymbol{f}_i \\ \boldsymbol{z}_i(t) = \sum\limits_{j\in\mathcal{N}_i} a_{ij}(\hat{\boldsymbol{x}}_j(t) - \hat{\boldsymbol{x}}_i(t) - (\boldsymbol{f}_j - \boldsymbol{f}_i)) + d_i(\hat{\boldsymbol{x}}_0(t) - \hat{\boldsymbol{x}}_i(t) + \boldsymbol{f}_i) \end{cases} \tag{4}$$

where $\boldsymbol{K} \in \mathbb{R}^{m\times n}$ is the gain of the feedback control, and $\boldsymbol{K}' \in \mathbb{R}^{m\times n}$ is the compensate gain to the formation variable. $\boldsymbol{z}_i(t)$ is the combinatory state. Define $\boldsymbol{z}(t) = [\boldsymbol{z}_1^T(t), \dots, \boldsymbol{z}_N^T(t)]^T$. For $\forall i \in \{1, \dots, N\}$, $\hat{\boldsymbol{x}}_i(t)$ is defined as:

$$\begin{cases} \hat{\boldsymbol{x}}_i(t_k^i) = \tilde{\boldsymbol{x}}_i(t_k^i) \\ \dfrac{d}{dt}\hat{\boldsymbol{x}}_i(t) = \boldsymbol{A}\hat{\boldsymbol{x}}_i(t) + \boldsymbol{B}\boldsymbol{K}'\boldsymbol{f}_i \end{cases}, \quad t \in [t_k^i, t_{k+1}^i) \tag{5}$$

where $\tilde{\boldsymbol{x}}_i(t_k^i)$ is the observer state at the last triggering moment t_k^i, which represents the kth ($k \in \mathbb{N}^+$) event of agent i. t_{k+1}^i is defined by event-triggered rules given in the following sections. Define measurement error of follower agent i as $\boldsymbol{e}_i(t) = \hat{\boldsymbol{x}}_i(t) - \tilde{\boldsymbol{x}}_i(t)$ and $\boldsymbol{e}(t) = [\boldsymbol{e}_1^T(t), \dots, \boldsymbol{e}_N^T(t)]^T$. Different from continuous control, $\hat{x}_i$ is sampled from the observer state $\tilde{x}_i$ at each event instant, and then $\hat{x}_i$ follows the rule defined in (5) until the next event instant. Note that the event-triggered mechanism is implemented during the agents' communication and also between the observer and the controller in each single agent.

The term $\hat{\boldsymbol{x}}_0(t)$ in (4) is defined as $\hat{\boldsymbol{x}}_i(t_k^0) = \tilde{\boldsymbol{x}}_i(t_k^0)$ and $\frac{d}{dt}\hat{\boldsymbol{x}}_0(t) = \boldsymbol{A}\hat{\boldsymbol{x}}_0(t)$ for $t \in [t_k^0, t_{k+1}^0)$. Note that, in practical engineering, the leader is usually specially chosen or a reference model and it can be treated independently. Therefore, it is reasonable to assume that its initial state is known, i.e., $\hat{\boldsymbol{x}}_0(0) = \tilde{\boldsymbol{x}}_0(0) = \boldsymbol{x}_0(0)$. Since the leader does not receive any input, the follower can estimate the leader's state using the equation $\hat{\boldsymbol{x}}_0(t) = e^{\boldsymbol{A}t}\hat{\boldsymbol{x}}_0(0) = e^{\boldsymbol{A}t}\boldsymbol{x}_0(0) = \boldsymbol{x}_0(t)$. Hence for brevity, we will regard $\hat{\boldsymbol{x}}_0(t)$ as $\boldsymbol{x}_0(t)$ in the rest of the paper.

Remark 1. The term $\hat{\boldsymbol{x}}_i(t) = \tilde{\boldsymbol{x}}_i(t_k^i)e^{\boldsymbol{A}(t-t_k^i)}$ is a model-based estimation [37]. Since the trivial static estimation $\hat{\boldsymbol{x}}_i(t) = \tilde{\boldsymbol{x}}_i(t_k^i)$ may differ from $\tilde{\boldsymbol{x}}_i(t)$ very quickly, the exponential term $e^{\boldsymbol{A}}$ with agent's dynamic matrix $\boldsymbol{A}$ is used to reduce the error between $\hat{\boldsymbol{x}}_i(t)$ and $\tilde{\boldsymbol{x}}_i(t)$ thus usually increases the inter-event time.

The objective of this paper is to design a DETM to determine the triggering moment t_k^i under the control law (4). The event-based data transmission process of agent i ($i \in \{1, \dots, N\}$) is described in Fig. 2: at the triggering moment t_k^i (where k represent the number of the most recent event of agent i), agent i broadcasts its current observed state $\tilde{\boldsymbol{x}}_i(t_k^i)$ to its downstream agents. Simultaneously, agent i updates the value of $\hat{\boldsymbol{x}}_i(t_k^i)$ to $\tilde{\boldsymbol{x}}_i(t_k^i)$. When agent i receives $\tilde{\boldsymbol{x}}_j(t_{k'}^j)$ from a neighbor agent j at agent j's triggering moments $t = t_{k'}^j$ (where k' represent the number of the most recent event of agent j), $\hat{\boldsymbol{x}}_j(t_{k'}^j)$ is updated to $\tilde{\boldsymbol{x}}_j(t_{k'}^j)$. When there is no event happens, the update of $\hat{\boldsymbol{x}}_i(t)$ or $\hat{\boldsymbol{x}}_j(t)$ follows the exponential law (5).

By the definition of $\boldsymbol{\delta}_i(t)$, $\boldsymbol{\zeta}_i(t)$ and $\boldsymbol{e}_i(t)$, one can deduce $\boldsymbol{z}_i(t)$ as

$$\boldsymbol{z}_i(t) = \sum_{j\in\mathcal{N}_i} a_{ij}(\boldsymbol{e}_j - \boldsymbol{e}_i + \boldsymbol{\zeta}_j - \boldsymbol{\zeta}_i + \boldsymbol{\delta}_j - \boldsymbol{\delta}_i) - d_i(\boldsymbol{e}_i + \boldsymbol{\zeta}_i + \boldsymbol{\delta}_i) \tag{6}$$

then one can obtain $\boldsymbol{z} = -(\boldsymbol{\mathcal{H}} \otimes \boldsymbol{I}_n)(\boldsymbol{e} + \boldsymbol{\zeta} + \boldsymbol{\delta})$ and the following expressions:

$$\begin{cases} \dot{\boldsymbol{\delta}} = (\boldsymbol{I}_N \otimes \boldsymbol{A} - \boldsymbol{\mathcal{H}} \otimes \boldsymbol{B}\boldsymbol{K})\boldsymbol{\delta} - (\boldsymbol{\mathcal{H}} \otimes \boldsymbol{B}\boldsymbol{K})(\boldsymbol{\zeta} + \boldsymbol{e}) + (\boldsymbol{I}_N \otimes (\boldsymbol{A} + \boldsymbol{B}\boldsymbol{K}'))\boldsymbol{f} \\ \dot{\boldsymbol{\zeta}} = (\boldsymbol{I}_N \otimes (\boldsymbol{A} + \boldsymbol{L}_o\boldsymbol{C}))\boldsymbol{\zeta} \\ \dot{\boldsymbol{e}} = (\boldsymbol{\mathcal{H}} \otimes \boldsymbol{B}\boldsymbol{K})\boldsymbol{\delta} + (\boldsymbol{I}_N \otimes \boldsymbol{A} + \boldsymbol{\mathcal{H}} \otimes \boldsymbol{B}\boldsymbol{K})\boldsymbol{e} + (\boldsymbol{\mathcal{H}} \otimes \boldsymbol{B}\boldsymbol{K} - \boldsymbol{I}_N \otimes \boldsymbol{L}_o\boldsymbol{C})\boldsymbol{\zeta} \end{cases} \tag{7}$$

The following assumptions hold in this paper:

Assumption 1. The communication topology between N follower agents is fixed and directed.

Assumption 2. The augmented graph $\bar{\mathcal{G}}$ contains a spanning tree with its root being the leader agent.

Assumption 3. $(\boldsymbol{A}, \boldsymbol{B}, \boldsymbol{C})$ is stabilizable and detectable.

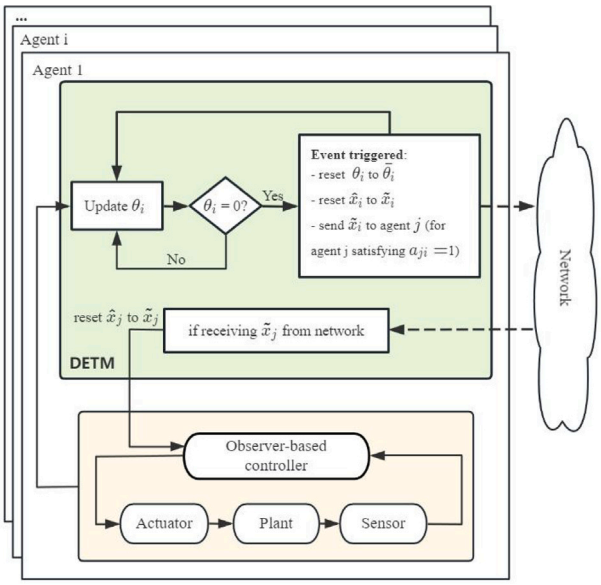

Fig. 2. DETM block diagram.

Recall the following property of matrix $\mathcal{H}$ due to [38] under Assumption 1 and Assumption 2:

Lemma 4. *There exists a positive diagonal matrix $\Psi = diag(\psi_1, \dots, \psi_N) > 0$ such that $\Psi\mathcal{H} + \mathcal{H}^T\Psi > 0$.*

4. Distributed DETM for leader-following formation control under directed topology

This section presents a comprehensive controller and observer design for the leader-following formation control problem under the DETM strategy.

4.1. Observer and controller synthesis

The following theorem proposes a distributed design of controllers and observers for follower agents and the DETM rule.

Theorem 5. *For the MAS described in (1), the leader-following formation will be achieved under the control law proposed in (4) if the following conditions are both satisfied:*

1. $(I_N \otimes (A + BK'))f = 0$
2. *The following $\mathcal{BMI}s$ are satisfied subject to $P_1 > 0$, $P_2 > 0$, the controller gain K and the observer gain L_o:*

$$S = \begin{pmatrix} S_{11} & S_{12} \\ * & S_{22} \end{pmatrix} < 0 \tag{8}$$

where S_{11}, S_{12} and S_{22} are defined as

$$\begin{cases} S_{11} = \Psi \otimes Sym(P_1A) - Sym((\Psi\mathcal{H}) \otimes (P_1BK)) \\ S_{12} = -(\Psi\mathcal{H}) \otimes (P_1BK) \\ S_{22} = \Psi \otimes Sym(P_2A + P_2L_oC) + (b_1 + b_2)I_{Nn} \end{cases} \tag{9}$$

with the matrix Ψ satisfying Lemma 4, and b_1, b_2 are two positive scalars. The event-triggered rule of agent i is defined as

$$t_{k+1}^i \triangleq \inf\left\{t > t_k^i \mid \theta_i(t) \le 0\right\}$$
$$\theta_i(t_k^i) = \bar{\theta}_i, \quad \dot{\theta}_i(t) = \begin{cases} \min(\omega_i(t), 0) - \tau_i & \text{if } \|e_i(t)\| \neq 0 \\ -\tau_i & \text{otherwise} \end{cases} \tag{10}$$

where $\bar{\theta}_i > 0$, $\tau_i > 0$, and $\omega_i(t)$ is defined as:

$$\omega_i(t) \triangleq -\frac{e_i^T\Pi_1 e_i + \Pi_2 z_i^T z_i + e_i^T\Pi_3 z_i}{\psi_i e_i^T P_3 e_i} \tag{11}$$

where

$$\begin{cases} \Pi_1 = \left(-\frac{\epsilon}{2} + k\|M\|^2 + \beta\right) I_n + 2\psi_i\theta_i P_3 A + \frac{1}{b_1}\gamma R_1 R_1^T + \frac{1}{b_2}\psi_i^2\theta_i^2 R_2 R_2^T \\ \Pi_2 = -\frac{\epsilon}{2}\bar{\delta}_{\min} + \frac{1}{k} \\ \Pi_3 = -2\psi_i\theta_i R_3 \end{cases} \tag{12}$$

and $R_1 = K^T B^T P_1$, $R_2 = P_3 L_o C$, $R_3 = P_3 BK$, $P_3 > 0$, $M = -\epsilon\mathcal{H}^{-1} \otimes I_n + 2(\mathcal{H}^T\Psi\mathcal{H}^{-1}) \otimes R_1$, $\bar{\delta}_{\min} = \lambda_{\min}(\mathcal{H}^{-T}\mathcal{H}^{-1})$, $\beta = \|Sym((\Psi\mathcal{H}) \otimes R_1^T)\|$, $\gamma = \|\Psi\mathcal{H}\|^2$, $k > 2/(\epsilon\bar{\delta}_{\min})$. The positive scalar $\epsilon > 0$ should satisfy $\epsilon \le \lambda_{\min}(-S)$.

Proof. The proof consists of showing the stability of the closed-loop system (7) based on Lyapunov theorem. One can choose the following Lyapunov function $V(t)$:

$$\begin{aligned} V(t) &= V_1(t) + V_2(t)t + V_3(t) \\ V_1(t) &= \delta(t)^T(\Psi \otimes P_1)\delta(t) \\ V_2(t) &= \zeta(t)^T(\Psi \otimes P_2)\zeta(t) \\ V_3(t) &= e(t)^T(\Psi\Theta(t) \otimes P_3)e(t) \end{aligned} \tag{13}$$

where $P_1, P_2, P_3 > 0$, $\Psi = \text{diag}(\psi_1, \dots, \psi_N)$ satisfying Lemma 4, $\Theta(t) = \text{diag}(\theta_1(t), \dots, \theta_N(t)) > 0$, and $\dot{\Theta}(t) < 0$ by definition of event-triggered rule (10), thus $V(t) \ge 0$. For the sake of brevity, the following text omits the part (t) for each variable.

Note that the Lyapunov function differs from that in [26] and can avoid the discontinuity phenomenon, as further discussed in Remark 4.

The derivatives of V_1, V_2, V_3 along the system trajectory are

$$\begin{cases} \dot{V}_1 = 2\delta^T(\Psi \otimes P_1A - \Psi\mathcal{H} \otimes R_1^T)\delta - 2\delta^T(\Psi\mathcal{H} \otimes R_1^T)e - 2\delta^T(\Psi\mathcal{H} \otimes R_1^T)\zeta \\ \dot{V}_2 = 2\zeta^T(\Psi \otimes P_2(A + L_oC))\zeta \\ \dot{V}_3 = 2e^T(\Psi\Theta \otimes P_3A + \Psi\Theta\mathcal{H} \otimes R_3)e + 2e^T(\Psi\Theta\mathcal{H} \otimes R_3 - \Psi\Theta \otimes R_2)\zeta \\ \qquad + 2e^T(\Psi\Theta\mathcal{H} \otimes R_3)\delta + e^T(\Psi\dot{\Theta} \otimes P_3)e \end{cases} \tag{14}$$

Lemma 4 shows that $\mathcal{H}$ is a M-matrix and its inverse $\mathcal{H}^{-1}$ is well-definite. By using the fact that $\delta = -(\mathcal{H}^{-1} \otimes I)z - e - \zeta$, then replace it in $\dot{V}_3$ and the term $-2\delta^T(\Psi\mathcal{H} \otimes R_1^T)e$ in $\dot{V}_1$ (14), one can obtain

$$\begin{aligned} \dot{V} =& \dot{V}_1 + \dot{V}_2 + \dot{V}_3 \\ =& 2\delta^T(\Psi \otimes P_1A - \Psi\mathcal{H} \otimes R_1^T)\delta \\ & - 2\delta^T(\Psi\mathcal{H} \otimes R_1^T)\zeta + 2\zeta^T(\Psi \otimes P_2(A + L_oC))\zeta \\ & + 2e^T(\mathcal{H}^T\Psi \otimes R_1 - \Psi\Theta \otimes R_2)\zeta \\ & + 2e^T(\mathcal{H}^T\Psi\mathcal{H}^{-1} \otimes R_1 - \Psi\Theta \otimes R_3)z \\ & + 2e^T(\Psi\Theta \otimes P_3A + \Psi\mathcal{H} \otimes R_1^T)e + e^T(\Psi\dot{\Theta} \otimes P_3)e \end{aligned} \tag{15}$$

Using Cauchy–Schwarz inequality, one can get

$$\begin{aligned} & 2e^T(\mathcal{H}^T\Psi \otimes R_1 - \Psi\Theta \otimes R_2)\zeta \\ \le & \frac{1}{b_1}e^T(\mathcal{H}^T\Psi^2\mathcal{H} \otimes R_1R_1^T)e + \frac{1}{b_2}e^T(\Psi\Theta^2\Psi \otimes R_2R_2^T)e \\ & + (b_1 + b_2)\zeta^T\zeta \end{aligned} \tag{16}$$

where b_1, b_2 are two strictly positive scalars. Then one can have

$$\begin{aligned} \dot{V} \le & 2\delta^T(\Psi \otimes P_1A - \Psi\mathcal{H} \otimes R_1^T)\delta - 2\delta^T(\Psi\mathcal{H} \otimes R_1^T)\zeta \\ & + 2\zeta^T(\Psi \otimes P_2(A + L_oC))\zeta + (b_1 + b_2)\zeta^T\zeta \\ & + \frac{1}{b_1}e^T(\mathcal{H}^T\Psi^2\mathcal{H} \otimes R_1R_1^T)e + \frac{1}{b_2}e^T(\Psi\Theta^2\Psi \otimes R_2R_2^T)e \\ & + 2e^T(\mathcal{H}^T\Psi\mathcal{H}^{-1} \otimes R_1 - \Psi\Theta \otimes R_3)z \\ & + 2e^T(\Psi\Theta \otimes P_3A + \Psi\mathcal{H} \otimes R_1^T)e + e^T(\Psi\dot{\Theta} \otimes P_3)e \end{aligned} \tag{17}$$

Since the internal state variables δ and ζ are not available in control system implementation, the idea is to guarantee $\dot{V}$ consistently negative with arbitrary δ and ζ. Notice that the first four terms in (17): $2\delta^T(\Psi\otimes P_1A-\Psi\mathcal{H}\otimes R_1^T)\delta-2\delta^T(\Psi\mathcal{H}\otimes R_1^T)\zeta+2\zeta^T(\Psi\otimes P_2(A+L_oC))\zeta+(b_1+b_2)\zeta^T\zeta$ form a quadratic expression with regard to δ and ζ, which could be written as $\xi^T S\xi$, with $\xi=(\delta^T\ \zeta^T)^T$ and S is defined in (9).

Since $S<0$ and $\epsilon\le\lambda_{\min}(-S)$, we have $\xi^T S\xi\le-\epsilon\|\xi\|^2=-\epsilon(\|\delta\|^2+\|\zeta\|^2)$. And notice that

$$-\epsilon(\|\delta\|^2+\|\zeta\|^2)\le-\epsilon\frac{(\delta+\zeta)^T(\delta+\zeta)}{2} \tag{18}$$

Substituting $z=-(\mathcal{H}\otimes I)(\delta+\zeta+e)\Rightarrow\delta+\zeta=-(\mathcal{H}^{-1}\otimes I)z-e$ in (18), one can obtain

$$\begin{aligned}&-\epsilon(\|\delta\|^2+\|\zeta\|^2)\\ \le&-\frac{\epsilon}{2}\left(z^T(\mathcal{H}^{-T}\otimes I_n)+e^T\right)\left((\mathcal{H}^{-1}\otimes I_n)z+e\right)\\ =&-\frac{\epsilon}{2}z^T\left(\mathcal{H}^{-T}\mathcal{H}^{-1}\otimes I_n\right)z-\frac{\epsilon}{2}e^Te-\epsilon e^T(\mathcal{H}^{-1}\otimes I_n)z\\ \le&-\frac{\epsilon}{2}\lambda_{\min}(\mathcal{H}^{-T}\mathcal{H}^{-1})z^Tz-\frac{\epsilon}{2}e^Te-\epsilon e^T(\mathcal{H}^{-1}\otimes I_n)z\end{aligned} \tag{19}$$

Let $\bar{\delta}_{\min}=\lambda_{\min}(\mathcal{H}^{-T}\ \mathcal{H}^{-1})$, then combining with (19) we have

$$\begin{aligned}&\delta^TS\delta\\ \le&-\epsilon(\|\delta\|^2+\|\zeta\|^2)\\ \le&-\frac{\epsilon}{2}\bar{\delta}_{\min}z^Tz-\frac{\epsilon}{2}e^Te-\epsilon e^T(\mathcal{H}^{-1}\otimes I_n)z\end{aligned} \tag{20}$$

Substituting (20) into (17), one can obtain

$$\begin{aligned}\dot{V}\le&-\frac{\epsilon}{2}\bar{\delta}_{\min}z^Tz-\frac{\epsilon}{2}e^Te\\&+\frac{1}{b_1}e^T(\mathcal{H}^T\Psi^2\mathcal{H}\otimes R_1R_1^T)e+\frac{1}{b_2}e^T(\Theta\Psi^2\Theta\otimes R_2R_2^T)e\\&+e^T(-\epsilon\mathcal{H}^{-1}\otimes I_n+2\mathcal{H}^T\Psi\mathcal{H}^{-1}\otimes R_1-2\Psi\Theta\otimes R_3)z\\&+2e^T(\Psi\Theta\otimes P_3A+\Psi\mathcal{H}\otimes R_1^T)e+e^T(\Psi\dot{\Theta}\otimes P_3)e\end{aligned} \tag{21}$$

This expression consists only of available information e (measurement errors) and z (control inputs). Define $M=-\epsilon\mathcal{H}^{-1}\otimes I_n+2\mathcal{H}^T\Psi\mathcal{H}^{-1}\otimes R_1$, $\beta=\|\mathrm{Sym}((\Psi\mathcal{H})\otimes R_1^T)\|$ and $\gamma=\|\Psi\mathcal{H}\|^2$, $k>2/(\epsilon\bar{\delta}_{\min})$. To obtain a distributed rule, the last step is to decouple the terms in (21) by using the following expressions:

$$\begin{cases}-\frac{\epsilon}{2}\bar{\delta}_{\min}z^Tz-\frac{\epsilon}{2}e^Te=-\frac{\epsilon}{2}\bar{\delta}_{\min}\sum_i z_i^Tz_i-\frac{\epsilon}{2}\sum_i e_i^Te_i\\ \frac{1}{b_1}e^T(\mathcal{H}^T\Psi^2\mathcal{H}\otimes R_1R_1^T)e\le\frac{1}{b_1}\gamma\sum_i e_i^TR_1R_1^Te_i\\ \frac{1}{b_2}e^T(\Theta\Psi^2\Theta\otimes R_2R_2^T)e\le\frac{1}{b_2}\sum_i\theta_i^2\psi_i^2e_i^TR_2R_2^Te_i\\ e^TMe\le k\|M\|^2\sum_i e_i^Te_i+\frac{1}{k}\sum_i z_i^Tz_i,\quad k>\frac{2}{\epsilon\bar{\delta}_{\min}}\\ e^T(-2\Psi\Theta\otimes R_3)z=-2\sum_i\psi_i\theta_ie_i^TR_3z_i\\ 2e^T(\Psi\Theta\otimes P_3A)e=2\sum_i\psi_i\theta_ie_i^TP_3Ae_i\\ 2e^T(\Psi\mathcal{H}\otimes R_1^T)e\le\beta\sum_i e_i^Te_i\\ e^T(\Psi\dot{\Theta}\otimes P_3)e=\sum_i\psi_i\dot{\theta}_ie_i^TR_2R_2^Te_i\end{cases} \tag{22}$$

Then (21) becomes

$$\dot{V}\le\sum_{i=1}^N\left(e_i^T\Pi_1e_i+\Pi_2z_i^Tz_i+e_i^T\Pi_3z_i+\dot{\theta}_i\psi_ie_i^TR_2R_2^Te_i\right) \tag{23}$$

where Π_1, Π_2, Π_3 are defined in (12). The lower bound of k is necessary for excluding Zeno effect, which will be shown in 6.

Enforcing each summation term (from $i=1$ to $i=N$) in (23) being negative and one can obtain that $\dot{\theta}_i(t)<\omega_i(t)$ with $\omega_i(t)$ defined in (11). One can also verify it by substituting (10) in (23) and we get $\dot{V}\le-\sum_i\tau_i<0$. Therefore, the closed-loop system (7) is asymptotically stable, and the MAS (1) achieves leader-following formation, which completes the proof.

Remark 2. Note that the design conditions of Theorem 5 are in bilinear form ($\mathcal{BMI}$ constraints), which are difficult to solve using existing numerical tools. Indeed, sufficient $\mathcal{LMI}$ design conditions for the existence of the proposed controller/observer are proposed below (see Corollary 7 and Corollary 9), which can be easily solved by numerical tools (such as YALMIP software).

Remark 3. Unlike the studies in [39,40], in the context of a directed topology, Eqs. (10) and (11) only necessitate the individual state of agent i, and the input variable z_i only depends on the states of each neighbor at their most recent event instant, as defined in Eq. (4). This design avoids the constraints in [39], where synchronization triggering between an agent and its neighbors is necessary, or in [40], where agent i needs to transmit control signals to its neighbors. Therefore, Eqs. (10) and (11) can effectively address the complexities brought by directed communication.

Remark 4. The Lyapunov function proposed in this proof is a continuous function, and the disadvantage of handling the discontinuous function in the study [26] is naturally avoided. Notice that $V_1(t)$ and $V_2(t)$ are continuous since $\delta(t)$ and $\zeta(t)$ are continuous. In V_3, the discontinuity of $e(t)$ and $\Theta(t)$ happens at the triggering agent. Suppose at $t=t_k^i$, agent i is triggered, thus we have $\lim_{t\to(t_k^i)^-}\theta_i(t)=0$, $\lim_{t\to(t_k^i)^+}\theta_i(t)=\bar{\theta}_i$, and $\lim_{t\to(t_k^i)^-}e_i(t)\ne0$, $\lim_{t\to(t_k^i)^+}e_i(t)=0$. Then we have

$$\lim_{t\to(t_k^i)^-}\psi_ie_i^T(t)\theta_i(t)P_3e_i(t)=\lim_{t\to(t_k^i)^+}\psi_ie_i^T(t)\theta_i(t)P_3e_i(t)=0 \tag{24}$$

Since $V_3=e^T(\Psi\Theta\otimes P_3)e=\sum_{i=1}^N\psi_ie_i^T(t)\theta_i(t)P_3e(t)$, it follows that

$$\lim_{t\to(t_k^i)^-}V_3(t)=\lim_{t\to(t_k^i)^+}V_3(t) \tag{25}$$

Therefore, it is proved that $V_3(t)$ is a continuous function, and thus $V(t)$ is also continuous.

Theorem 5 imposes $(I_N\otimes(A+BK'))f=0$ as the formability condition which depends not only on formation variables but also on system's dynamic. Similar conditions have also been proposed in [15], and the formation variable f could not be arbitrarily chosen to have a feasible solution K'. However, the gain matrix K' may be unnecessary for systems with some properties, e.g., for single-integrator systems with $A=0$, we can choose $K'=0$ and arbitrary f.

The main difficulty lies in determining K and L_o, which involves a set of $\mathcal{BMI}s$ (9). These equations can be numerically challenging to solve. In order to facilitate computation, these $\mathcal{BMI}s$ are transformed to $\mathcal{LMI}s$ in Section 4.3.

4.2. Designable minimum inter-event time

The following corollary presents an explicit expression of MIET and proves that the Zeno behavior does not exist under Theorem 5.

Corollary 6. *The MAS described in (1) achieves leader-following formation under Theorem 5 with the inter-event time of agent i is lower-bounded by $t_{\min}^i$ defined as*

$$t_{\min}^i=\int_0^{\bar{\theta}_i}\frac{1}{\max(c_0+c_1h+c_2h^2,0)+\tau_i}\mathrm{d}h \tag{26}$$

where

$$\begin{cases}c_0=\dfrac{-\epsilon/2+k\|M\|^2+\beta+\gamma\|R_1\|^2/b_1}{\psi_i\eta}\\ c_1=\dfrac{\alpha}{\eta}\\ c_2=\dfrac{1}{\eta}\left(\dfrac{\psi_i\|R_2\|^2}{b_2}+\dfrac{\|R_3\|^2}{\sigma}\right)\end{cases} \tag{27}$$

and $\alpha = \lambda_{\max}(Sym(\boldsymbol{P}_3\boldsymbol{A}))$, $\beta = \|Sym(\boldsymbol{\Psi}\boldsymbol{\mathcal{H}} \otimes \boldsymbol{R}_1^T)\|$, $\gamma = \|\boldsymbol{\Psi}\boldsymbol{\mathcal{H}}\|^2$, $\eta = \lambda_{\min}(\boldsymbol{P}_3)$, $k > 2/(\epsilon\bar{\delta}_{\min})$, *the constants* τ_i, ψ_i, ϵ, b_1, b_2 *are defined in Theorem 5, and* σ *is a strictly positive scalars satisfying* $\frac{\epsilon\bar{\delta}_{\min}}{2} - \frac{1}{k} - \psi_i\sigma = 0$.

Proof. See Appendix A

Remark 5. Corollary 6 implies that the Zeno behavior of the proposed DETM is excluded. By adjusting the value of $\bar{\theta}_i$, we can vary the MIET and keep the communication frequency consistently lower than $1/t^i_{\min}$, and there also exists an upper bound for $t^i_{\min}$. Increasing the value of $\bar{\theta}_i$ enables the inter-event time as long as possible to not overload the communication network, which will also lead to a longer time to converge. Indeed, a smaller $\bar{\theta}_i$ could also be designed to keep better surveillance and a faster formation speed. In fact, the performance degradation caused by the DETM is minor, which is demonstrated in the simulation part 5.3. Therefore, by choosing an appropriate parameter $\bar{\theta}_i$, the control performance and the communication frequency could achieve a good compromise.

Remark 6. Compared with the existing literature [23,24], where the relationship between the MIET and the system matrix is complex, the result in Corollary 6 is clearer and more concise. As $t^i_{\min}$ can be regarded as a function of the scalar $\bar{\theta}_i$, MIETs are also decoupled for each agent. Therefore, under the distributed control architecture, one can independently determine the MIET for each agent.

Remark 7. One can calculate $t^i_{\min}$ through either numerical integration, or analytical integration if $c_0 + c_1 h + c_2 h^2 \geq 0$, $\forall h \in [0, \bar{\theta}_i]$. In the second case, the analytical integration depends on the roots (could be complex number) of $(c_0 + \tau_i) + c_1 h + c_2 h^2 = 0$, which are denoted as h_1 and h_2. Notice that c_0, c_1, c_2 are all positive in this case and $(c_0 + \tau_i) + c_1 h + c_2 h^2 > 0$, then $t^i_{\min}$ can be written in (28).

$$t^i_{\min} = \begin{cases} \dfrac{1}{c_2(h_1 - h_2)} \ln\left(\dfrac{h_2(\bar{\theta}_i - h_1)}{h_1(\bar{\theta}_i - h_2)}\right) & \text{if } \Delta > 0 \\ -\dfrac{1}{c_2}\left(\dfrac{1}{h_1} + \dfrac{1}{\bar{\theta}_i - h_1}\right) & \text{if } \Delta = 0 \\ \dfrac{2}{\sqrt{-\Delta}}\left[\arctan\left(\dfrac{2c_2}{\sqrt{-\Delta}}\bar{\theta}_i + \dfrac{c_1}{\sqrt{-\Delta}}\right) - \arctan\left(\dfrac{c_1}{\sqrt{-\Delta}}\right)\right] & \text{if } \Delta < 0 \end{cases} \tag{28}$$

where $\Delta = c_1^2 - 4c_2(c_0 + \tau_i)$. Note that $t^i_{\min}$ could be regarded as a function of $\bar{\theta}_i$ and one can also obtain the maximum value of $t^i_{\min}$ as $(t^i_{\min})_{\max} = \max_{\bar{\theta}_i > 0} t^i_{\min}$:

$$(t^i_{\min})_{\max} = \begin{cases} \dfrac{1}{\sqrt{\Delta}} \ln \dfrac{c_1 + \sqrt{\Delta}}{c_1 - \sqrt{\Delta}} & \text{if } \Delta > 0 \\ \dfrac{2}{c_1} & \text{if } \Delta = 0 \\ \dfrac{2}{\sqrt{-\Delta}}\left[\dfrac{\pi}{2} - \arctan\left(\dfrac{c_1}{\sqrt{-\Delta}}\right)\right] & \text{if } \Delta < 0 \end{cases} \tag{29}$$

4.3. LMI-based sufficient conditions

Solving the $\mathcal{BMI}s$ in Theorem 5 could be challenging and may require many attempts through numerical iterations. In order to address this issue, $\mathcal{LMI}$ conditions are proposed in the following Corollary 7 and Corollary 9.

Corollary 7. *The MAS (1) will achieve the leader-following formation under the control law (4) and the DETM proposed in (10) if the following conditions are both satisfied:*

1. $(\boldsymbol{I}_N \otimes (\boldsymbol{A} + \boldsymbol{B}\boldsymbol{K}'))\boldsymbol{f} = \boldsymbol{0}$,
2. *There exists matrices* $\boldsymbol{P}_1 > 0$, $\boldsymbol{P}_2 > 0$, $\boldsymbol{K}$ *and* $\boldsymbol{F}$ *such that the following* $\mathcal{LMI}s$ *hold:*

$$\begin{cases} \boldsymbol{\Omega} = \begin{pmatrix} \boldsymbol{\Omega}_{11} & \boldsymbol{0}_{Nn} & (\boldsymbol{\Psi}\boldsymbol{\mathcal{H}}) \otimes (\boldsymbol{P}_1\boldsymbol{B}) & \boldsymbol{\Omega}_{14} \\ * & \boldsymbol{\Omega}_{22} & -\boldsymbol{I}_N \otimes \boldsymbol{K}^T & \boldsymbol{0}_{Nn} \\ * & * & -2\boldsymbol{I}_{Nm} & \boldsymbol{0}_{Nm\times Nn} \\ * & * & * & -\boldsymbol{I}_{Nn} \end{pmatrix} < 0 \\ \boldsymbol{\Omega}_{11} = \boldsymbol{\Psi} \otimes (Sym(\boldsymbol{P}_1\boldsymbol{A})) + \boldsymbol{I}_{Nn} - 2\dfrac{\boldsymbol{I}_N \otimes \boldsymbol{P}_1}{\mu_1} \\ \boldsymbol{\Omega}_{14} = \dfrac{\boldsymbol{I}_N \otimes \boldsymbol{P}_1}{\mu_1} - \mu_1(\boldsymbol{\Psi}\boldsymbol{\mathcal{H}}) \otimes (\boldsymbol{K}^T\boldsymbol{B}^T) \\ \boldsymbol{\Omega}_{22} = \boldsymbol{\Psi} \otimes (Sym(\boldsymbol{P}_2\boldsymbol{A} + \boldsymbol{F}\boldsymbol{C})) + (b_1 + b_2)\boldsymbol{I}_{Nn} \end{cases} \tag{30}$$

where the matrix $\boldsymbol{\Psi}$ *satisfying Lemma 4,* b_1, b_2, μ_1 *are arbitrary strictly positive scalars. Then the gain of observer is obtained as* $\boldsymbol{L}_o = \boldsymbol{P}_2^{-1}\boldsymbol{F}$ *and the gain of controller is obtained as the matrix* $\boldsymbol{K}$. *This* $\mathcal{LMI}s$ *with* $\boldsymbol{P}_1$, $\boldsymbol{P}_2$, $\boldsymbol{K}$ *and* $\boldsymbol{F}$ *become a sufficient condition for* $\mathcal{BMI}s$ $\boldsymbol{S} < 0$ *in (9) and the positive scalar* $\epsilon > 0$ *in (10) should satisfy* $\epsilon \leq \lambda_{\min}(-\boldsymbol{S})$.

Proof. See Appendix B.

The following corollary proposes another $\mathcal{LMI}$ formulation which leads to less conservative results than Corollary 7. Consider the following assumption:

Assumption 8. The matrix $\boldsymbol{B}$ has full column rank.

Remark 8. This property in Assumption 8 is commonly observed in autonomous systems such as quadrotors, VTOL aircraft, fixed-wing aircraft, and autonomous ground vehicles. It implies that the dimension of the input space is larger than that of the state space, i.e., $m \leq n$, and the columns of $\boldsymbol{B}$ are linearly independent. However, it is important to carefully examine the matrix $\boldsymbol{B}$, particularly in dealing with over-actuated systems.

Corollary 9. *The MAS (1) will achieve the leader-following formation under the control law (4) and the DETM proposed in (10) if the following conditions are both satisfied:*

1. $(\boldsymbol{I}_N \otimes (\boldsymbol{A} + \boldsymbol{B}\boldsymbol{K}'))\boldsymbol{f} = \boldsymbol{0}$,
2. *There exists matrices* $\boldsymbol{P}_1 > 0$, $\boldsymbol{P}_2 > 0$, $\boldsymbol{N}$, $\boldsymbol{R}$ *and* $\boldsymbol{F}$ *such that the following* $\mathcal{LMI}s$ *hold:*

$$\begin{cases} \boldsymbol{\Xi} = \begin{pmatrix} \boldsymbol{\Xi}_{11} & \boldsymbol{\Xi}_{12} \\ * & \boldsymbol{\Xi}_{22} \end{pmatrix} < 0 \\ \boldsymbol{\Xi}_{11} = \boldsymbol{\Psi} \otimes (Sym(\boldsymbol{P}_1\boldsymbol{A})) - Sym((\boldsymbol{\Psi}\boldsymbol{\mathcal{H}}) \otimes (\boldsymbol{B}\boldsymbol{N})) \\ \boldsymbol{\Xi}_{12} = -(\boldsymbol{\Psi}\boldsymbol{\mathcal{H}}) \otimes (\boldsymbol{B}\boldsymbol{N}) \\ \boldsymbol{\Xi}_{22} = \boldsymbol{\Psi} \otimes (Sym(\boldsymbol{P}_2\boldsymbol{A} + \boldsymbol{F}\boldsymbol{C})) + (b_1 + b_2)\boldsymbol{I}_{Nn} \\ \boldsymbol{B}\boldsymbol{R} = \boldsymbol{P}_1\boldsymbol{B} \end{cases} \tag{31}$$

where the matrix $\boldsymbol{\Psi}$ *satisfying Lemma 4,* b_1, b_2 *are two arbitrary positive scalar. Then* $\boldsymbol{K}, \boldsymbol{L}_o$ *are obtained as* $\boldsymbol{K} = \boldsymbol{R}^{-1}\boldsymbol{N}$, $\boldsymbol{L}_o = \boldsymbol{P}_2^{-1}\boldsymbol{F}$. $\boldsymbol{P}_1$, $\boldsymbol{P}_2$, $\boldsymbol{K}$ *and* $\boldsymbol{F}$ *are also a set of solution for* $\mathcal{BMI}s$ $\boldsymbol{S} < 0$ *in (9) and the positive scalar* $\epsilon > 0$ *in (10) should satisfy* $\epsilon \leq \lambda_{\min}(-\boldsymbol{S})$.

Proof. See Appendix C.

Remark 9. It is worth noting that Corollary 9 is derived from equality constraints and is comparatively less conservative than Corollary 7. This is due to the local linear approximation of the quadratic term $-\frac{\boldsymbol{I}_N \otimes \boldsymbol{P}_1^2}{\mu_1^2}$ by using a linear upper bound $\boldsymbol{I}_{Nn} - 2\frac{\boldsymbol{I}_N \otimes \boldsymbol{P}_1}{\mu_1}$ in (B.4). It should be noted that matrix $\boldsymbol{A}$ may be non-Hurwitz, which further reduces the feasible solution space, indicating that these $\mathcal{LMI}s$ in

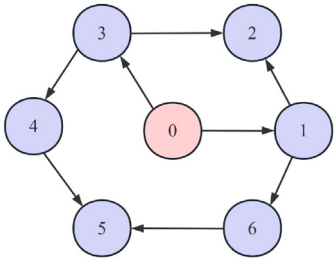

Fig. 3. Communication topology.

Corollary 7 are conservative then Corollary 9. On the contrary, based on Assumption 8, the equality constraint $\boldsymbol{BR} = \boldsymbol{P}_1\boldsymbol{B}$ used in (31) is used without introducing new conservatism, which preserves the quality of the result compared to the basic result of Theorem 5.

5. Numerical examples and discussions

Consider a MAS with six follower agents and one leader. These agents present wheeled mobile robots. Denote the state vector $\boldsymbol{x}_i = [p_i^x \ p_i^y \ v_i^x \ v_i^y]^T$ where p_i^x, p_i^y are the position components along X and Y axes, and v_i^x, v_i^y are the linear velocity components along X and Y axes. The system dynamics are defined in (1) with the following matrices:

$$\boldsymbol{A} = \begin{pmatrix} 0 & 0 & 1 & 0 \\ 0 & 0 & 0 & 1 \\ 0 & 0 & 0 & 0 \\ 0 & 0 & 0 & 0 \end{pmatrix}, \boldsymbol{B} = \begin{pmatrix} 0 & 0 \\ 0 & 0 \\ 1 & 0 \\ 0 & 1 \end{pmatrix}, \boldsymbol{C} = \begin{pmatrix} 1 & 0 & 0 & 0 \\ 0 & 1 & 0 & 0 \end{pmatrix} \tag{32}$$

This type of dynamic is widely used to describe mobile robots, such as in [15,32], and notice that the matrix $\boldsymbol{B}$ has full column rank. The agents' initial conditions are set as $\boldsymbol{x}_0(0) = [0\ 0\ 0.5\ 0]^T$, $\boldsymbol{x}_1(0) = [-2\ 0\ 0\ 0]^T$, $\boldsymbol{x}_2(0) = [0\ 2\ 0\ 0]^T$, $\boldsymbol{x}_3(0) = [0\ 1\ 0.1\ 0]^T$, $\boldsymbol{x}_4(0) = [2\ 2\ 0\ 0]^T$, $\boldsymbol{x}_5(0) = [0\ -2\ 0\ 0.1]^T$, $\boldsymbol{x}_6(0) = [2\ -2\ 0\ 0]^T$. The initial states of observers are set as 0. Consider a hexagon formation and the formation variables are chosen as $\boldsymbol{f}_1 = [1\ 0\ 0\ 0]^T$, $\boldsymbol{f}_2 = [0.5\ \sqrt{3}/2\ 0\ 0]^T$, $\boldsymbol{f}_3 = [-0.5\ \sqrt{3}/2\ 0\ 0]^T$, $\boldsymbol{f}_4 = [-1\ 0\ 0\ 0]^T$, $\boldsymbol{f}_5 = [-0.5\ -\sqrt{3}/2\ 0\ 0]^T$, $\boldsymbol{f}_6 = [0.5\ -\sqrt{3}/2\ 0\ 0]^T$. In this scenario, we can choose $K' = \boldsymbol{0}$ and verify that $(\boldsymbol{I}_N \otimes (\boldsymbol{A} + \boldsymbol{BK}'))\boldsymbol{f} = 0$ in Theorem 5.

Consider a directed communication topology described in Fig. 3. The corresponding augmented graph $\bar{\mathcal{G}}$ contains a spanning tree, and the leader agent is the root, which satisfies Assumption 2. The matrix $\boldsymbol{\Psi}$ calculated is $\boldsymbol{\Psi} = \mathrm{diag}(9.10\ 3.62\ 9.10\ \ 6.76\ 3.46\ 6.76)$.

Since the control input matrix $\boldsymbol{B}$ has full column rank, this example compares the result by using Corollary 9 and Corollary 7 with $b_1 = b_2 = 1$ and obtains the following solution in Table 1. Note that in this simulation setting, Corollary 7 finds no solution for the LMIs (11), while Corollary 9 can still give a good result, which shows that 9 is less conservative.

Remark 10. For practical engineering, constraints can be added to assign the eigenvalues of the observer dynamic $\boldsymbol{A} + \boldsymbol{L}_o\boldsymbol{C}$. The pole placement technique is considered valid as long as the corresponding matrix $\boldsymbol{S}$ in (8) is negative definite. By implementing this approach, the convergence performance of the observer can be adjusted to meet the desired requirements.

5.1. Formation behavior

Select $\epsilon = 0.1$ to satisfy $\epsilon \le \lambda_{\min}(-\boldsymbol{S})$. Set $\boldsymbol{P}_3 = \boldsymbol{P}_1$. Set the initial value of ADVs as $\bar{\theta}_i = 10, i = 1, \ldots, 6$. The trajectories of formation error and observer state error are depicted in Fig. 4 and Fig. 5, respectively. It can be seen that the formation is well achieved. The consensus error and the observer error asymptotically diminish over time, indicating

Table 1
Numerical results using Corollary 9 and Corollary 7.

	Corollary 9	Corollary 7
$\boldsymbol{P}_1$	$\begin{pmatrix} 0.0226 & 0.0000 & 0.0781 & 0.0000 \\ 0.0000 & 0.0226 & 0.0000 & 0.0781 \\ 0.0781 & 0.0000 & 0.9487 & 0.0000 \\ 0.0000 & 0.0781 & 0.0000 & 0.9487 \end{pmatrix}$	
$\boldsymbol{P}_2$	$\begin{pmatrix} 11.4383 & 0.0200 & -1.4482 & 0.0169 \\ 0.0200 & 11.4673 & -0.0165 & -1.4550 \\ -1.4482 & -0.0165 & 11.3689 & -0.0002 \\ 0.0169 & -1.4550 & -0.0002 & 11.4118 \end{pmatrix}$	No solution
$\boldsymbol{K}$	$\begin{pmatrix} 0.0781 & 0.0000 & 0.9487 & 0.0000 \\ 0.0000 & 0.0781 & 0.0000 & 0.9487 \end{pmatrix}$	
$\boldsymbol{L}_o$	$\begin{pmatrix} -1.4000 & 0.0000 & -9.4900 & 0.0000 \\ 0.0000 & -1.0000 & 0.0000 & -1.2500 \end{pmatrix}^T$	

that the agents are effectively coordinating their actions and aligning their states to achieve a collective objective. This outcome validates the effectiveness of our control strategy in driving the system toward a desired formation. Fig. 6 displays the relative displacement of each follower agent, where some snapshots are shown in Fig. 7. $\bar{p}_i^x$ and $\bar{p}_i^y$ are the positions of agents relative to the leader, which are defined as $\bar{p}_i^x = p_i^x - p_0^x$ and $\bar{p}_i^y = p_i^y - p_0^y$, where p_0^x and p_0^y are the x-axis and y-axis position components of the leader. Fig. 8 illustrates the corresponding control input of each agent.

Fig. 9 and Fig. 10 present the time evolution of $\theta_i(t)$ and $\boldsymbol{e}_i(t)$, respectively. As shown, the behavior of $\theta_i(t)$ (resp. $\boldsymbol{e}_i(t)$) for each agent is asynchronous, with events occurring at the discontinuous points where $\theta_i(t)$ (resp. $\boldsymbol{e}_i(t)$) is reset to $\bar{\theta}_i$ (resp. 0), indicating a clock-like behavior. This phenomenon of asynchronization arises due to the distributed nature of the multi-agent system, where each agent operates independently based on its local information and interactions with neighboring agents.

5.2. Inter-event time

Fig. 11 displays the event-triggered instants for each agent within 45 s. The event density varies with time, with a higher frequency of events during the initial stage (first 10 s) than when the system is stable (after approximately 20 s). In the initial phase, the relatively dense lattice is actually a result of the scale of the x-axis. After zooming in the interval from 0 to 3 s, it becomes evident that the lattice remains relatively dispersed. For instance, in the first 1 s, there are 11 events for agent 3, resulting in an event frequency of 11 Hz. This frequency notably falls below a common control rate or communication, such as the typical 50–200 Hz range in drones or other UAV control systems. This is also evident from Fig. 12, which shows a longer inter-event time during the later stage compared to the beginning stage, avoiding unnecessary utilization of resources.

Note that events exhibit greater density during the initial phase (approximately the first 10 s) compared to the stable phase (after $t = 20$ s). This phenomenon arises from the relatively larger errors during the initial phase, leading to shorter inter-event intervals under the event rule (10). Intuitively, agents have more frequent communication when dealing with non-consensus states and large formation errors, which can result in rapid error accumulation and eventual instability. Conversely, during the stable phase (after $t = 20$ s) when formation errors are minor, rapid information exchange is no longer required, and thus we have more sparse events.

In order to decrease the communication frequency, we can adjust the $\bar{\theta}_i$ for each agent to tune the corresponding inter-event time. For example, we change the $\bar{\theta}_4$ of agent 4, and maintain $\bar{\theta}_i = 10$ of other agents $i \neq 4$. The inter-event time of agent 4 is correspondingly modified as can be seen in Fig. 13.

Furthermore, we change $\bar{\theta}_i$, $i = 1, \ldots, 6$ for all agents and present the inter-event time in Table 2, together with the static event-triggered

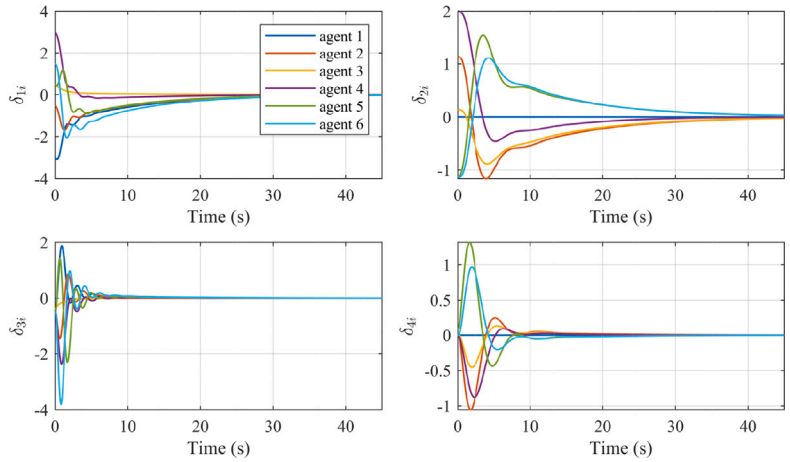

Fig. 4. Formation error of follower agents. δ_{ji} denotes the jth dimension of agent i's formation error. ($\bar{\theta}_i = 10,\ i = 1, \ldots, 6$).

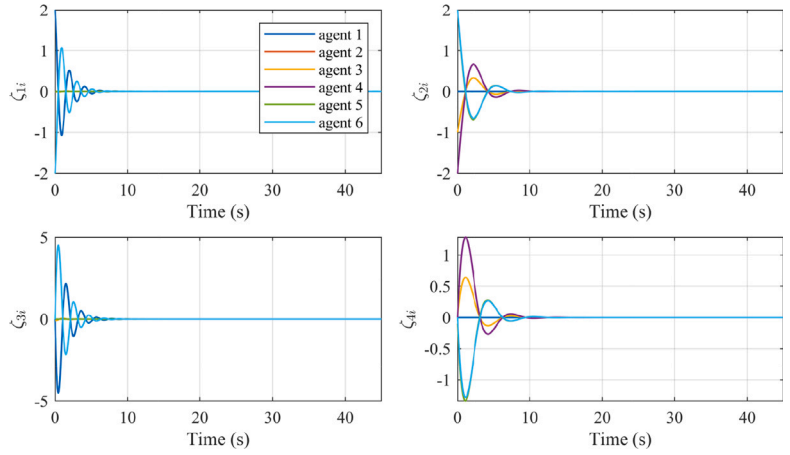

Fig. 5. Observer state error of follower agents. ζ_{ji} denotes the jth dimension of agent i's observer state error. ($\bar{\theta}_i = 10,\ i = 1, \ldots, 6$).

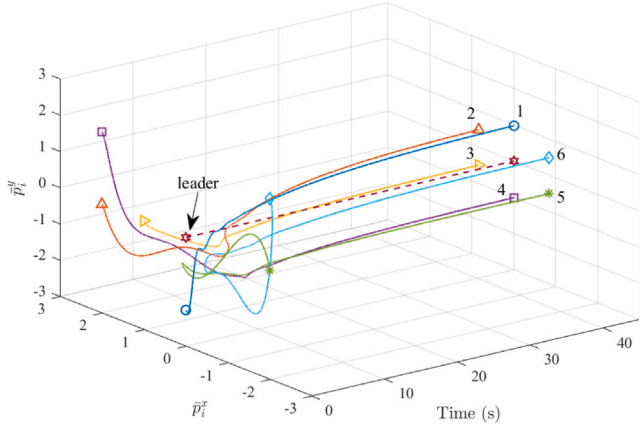

Fig. 6. Trajectory of relative displacement of follower agents to the leader. $\bar{p}_i^x = p_i^x - p_0^x$ and $\bar{p}_i^y = p_i^y - p_0^y$, where p_0^x and p_0^y are the x-axis and y-axis position components of the leader. ($\bar{\theta}_i = 10,\ i = 1, \ldots, 6$).

mechanism (SETM). For SETM, the Lyapunov function is the same as in the proof of Theorem 5 by taking $\boldsymbol{\Theta} = \boldsymbol{I}_N, \dot{\boldsymbol{\Theta}} = \boldsymbol{0}$, which finally leads to a static event-triggered rule. According to this table, the inter-event time increases with larger $\bar{\theta}_i$ and can be easily tuned to be longer than SETM. Hence, by appropriately adjusting $\bar{\theta}_i$, the IET can be tailored to meet specific requirements, which highlights the notable advantage of the proposed method compared to the existing SETM.

Table 2
Inter-event time (in ms) using different $\bar{\theta}_i$ under proposed DETM strategy and static event-triggered mechanism (SETM): mean values (Mean), minimum values (Min) and maximum values (Max) among 6 follower agents.

Case		Mean	Min	Max
DETM	$\bar{\theta}_i = 0.5$	121.9	1.626	500.0
	$\bar{\theta}_i = 1$	243.8	9.431	1001
	$\bar{\theta}_i = 10$	315.5	9.948	1486
	$\bar{\theta}_i = 100$	318.7	10.39	1497
	$\bar{\theta}_i = 500$	320.7	10.42	1471
SETM		40.67	1.000	865.0
Ref [26]		unguaranteed consensus		
Periodic communication		1.000		

In Fig. 14, $t^i_{\min}$ is plotted with different values of $\bar{\theta}_i$ using (26). The proposed DETM method can prevent Zeno behavior as long as $\bar{\theta}_i > 0$. By adjusting $\bar{\theta}_i$, we can control the MIET and ensure that network communication remains consistently below a designated frequency. It should be noted that $t^i_{\min}$ is only a lower bound on the inter-event time and the actual average inter-event time, as shown in Table 2, is much longer than the MIET, which serves only as an indicator in the worst case scenario.

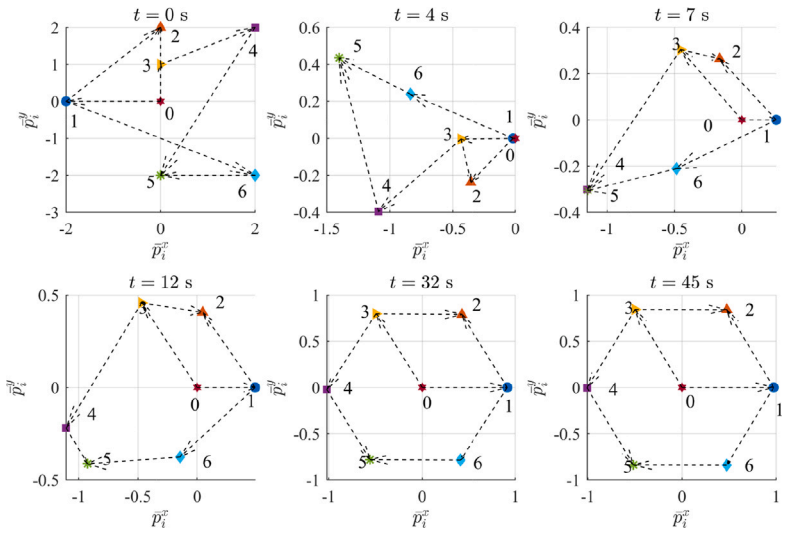

Fig. 7. Position snapshots of agents at $t = 0$ s, $t = 4$ s, $t = 7$ s, $t = 12$ s, $t = 32$ s, and $t = 45$ s. Dashed arrows denote the communication topology. $\bar{p}_i^x = p_i^x - p_0^x$ and $\bar{p}_i^y = p_i^y - p_0^y$, where p_0^x and p_0^y are the position components of the leader. ($\bar{\theta}_i = 10,\ i = 1, \ldots, 6$).

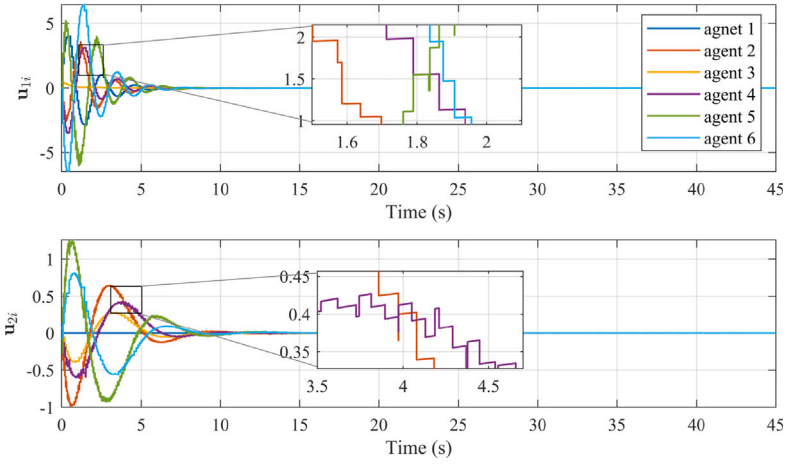

Fig. 8. Control input of follower agents. u_{ji} denotes the jth dimension of agent i's control input. ($\bar{\theta}_i = 10,\ i = 1, \ldots, 6$).

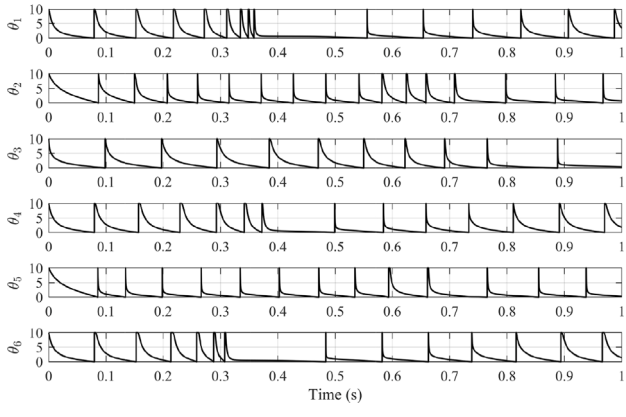

Fig. 9. Time evolution of auxiliary dynamic variables $\theta_i(t)$ of follower agents. ($\bar{\theta}_i = 10,\ i = 1, \ldots, 6$).

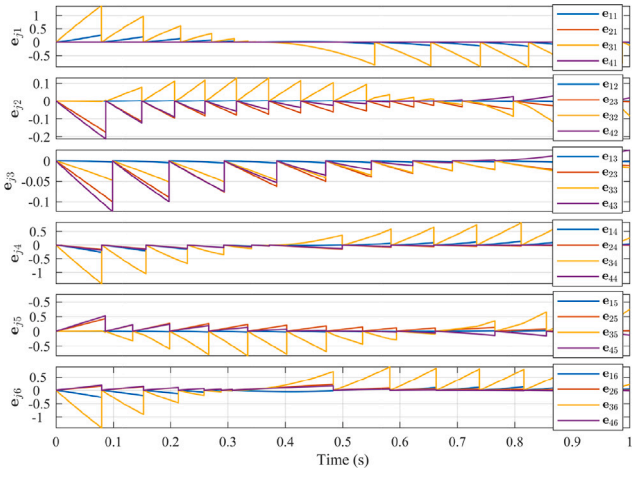

Fig. 10. Measurement error of follower agents. e_{ji} denotes the jth dimension of agent i's measurement error. ($\bar{\theta}_i = 10,\ i = 1, \ldots, 6$).

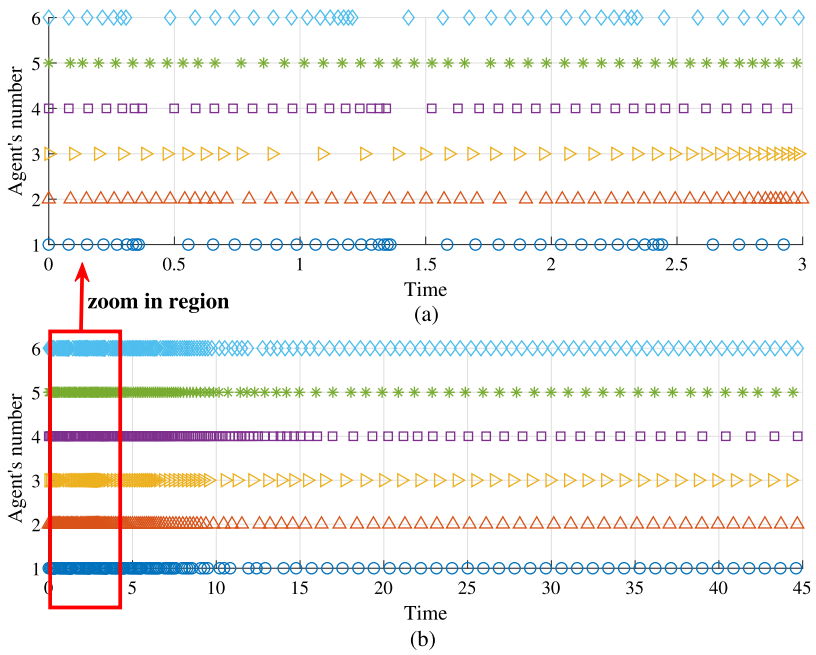

Fig. 11. (a) Event-triggered instants of follower agents during initial stage $t \in [0, 3]$. (b) Event-triggered instants of follower agents $t \in [0, 45]$ ($\bar{\theta}_i = 10,\ i = 1, \ldots, 6$).

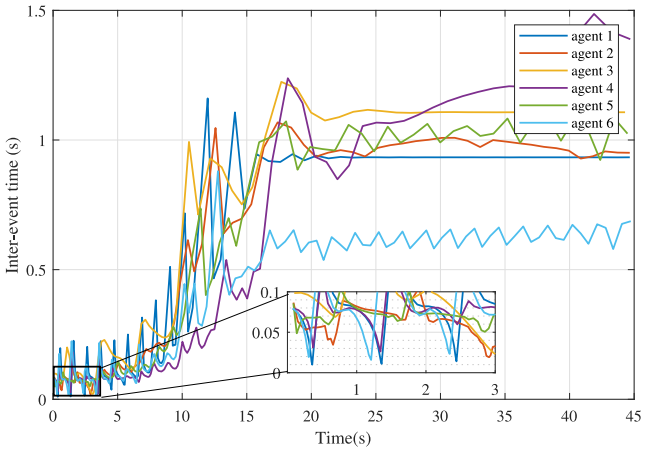

Fig. 12. Inter-event time of follower agents. ($\bar{\theta}_i = 10,\ i = 1, \ldots, 6$).

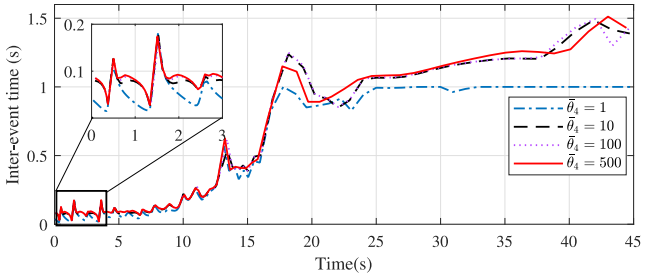

Fig. 13. Inter-event time of agent 4 with different $\bar{\theta}_4$ ($\bar{\theta}_i = 10,\ i \neq 4$).

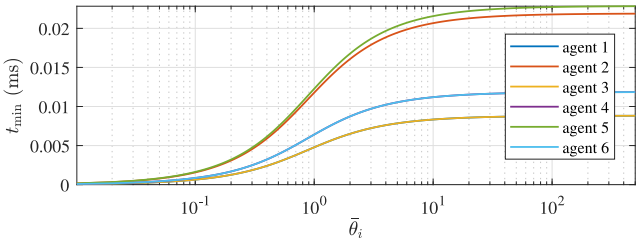

Fig. 14. Minimum inter-event time $t^i_{\min}$ with different $\bar{\theta}_i$ using (26).

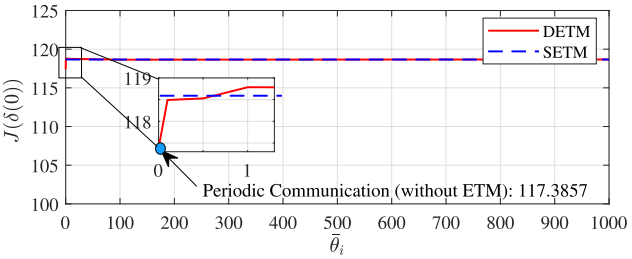

Fig. 15. Quadratic Integral Performance (33) with different value of $\bar{\theta}_i$.

5.3. Discussion on the performance

In order to examine the influence of parameters $\bar{\theta}_i$ on the performance, we use the following quadratic integral index of the closed loop system [17]:

$$J(\boldsymbol{\delta}(0)) = \sum_{i=1}^{N} \int_0^{t_{\text{final}}} \boldsymbol{\delta}_i(t)^T \boldsymbol{Q} \boldsymbol{\delta}_i(t) \mathrm{d}t \tag{33}$$

where $\boldsymbol{Q} > 0$. In Table 3, $J(\boldsymbol{\delta}(0))$ are analyzed in relation to distinct values of $\bar{\theta}_i$ and static ETM strategy. The outcome shows that $\bar{\theta}_i$ will increase $J(\boldsymbol{\delta}(0))$, and this similar behavior has also been found in [17]. However, compared to the periodic communication without any ETM, this increment of performance index is marginal. In this case, it is reasonable to set a larger $\bar{\theta}_i$ for a longer inter-event time (see Table 2 and Fig. 14), and meanwhile with minor performance degradation. Fig. 15 also corroborates this finding, with the performance index of the DETM (with a large $\bar{\theta}_i$) closed to the SETM. Such a small change of $J(\boldsymbol{\delta}(0))$ could be regarded as a light impact on the performance, and we could also have a much longer inter-event time as well as reduce the usage of network resources.

Table 3
Quadratic Integral Performance (33) by using different strategies and performance degradation percentage compared to the periodic communication. (Periodic communication: communication interval=1ms, without any ETM).

Case	DETM $\bar{\theta}_i,\ i=1,\dots,6$					SETM	Periodic communication
$\bar{\theta}_i$	0.5	1	10	100	500		
$J(\delta(0))$	118.5273	118.7854	118.7470	118.6407	118.6536	118.661	117.3857
Performance degradation percentage	0.97%	1.19%	1.16%	1.07%	1.08%	1.09%	0%

6. Conclusion

This paper presents an innovative solution to the leader-following formation problem in MASs under directed topology. The proposed approach aims to reduce the frequency of inter-agent information exchange by implementing a dynamic event-triggered control protocol. This protocol allows for the design of the inter-event time, and an explicit expression for the minimum inter-event time is provided, which enables more flexible tuning and prevents Zeno behavior. Model-based estimation and clock-like auxiliary dynamic variables are introduced in the proposed methods to prolong the inter-event time. The co-design of distributed controllers and observers is synthesized by $\mathcal{BMI}s$, which is eventually simplified to $\mathcal{LMI}s$ and further distinguishes this study. Simulation results demonstrate a significant improvement compared to the existing static event-triggered control, showcasing the effectiveness of the proposed solution. The degradation of quadratic integral performance is shown to be marginal, while it leads to a longer inter-event time. Our further works will focus on extending the proposed methods for MASs subject to faults and switching topology under external disturbances and system uncertainties, which are also important aspects of practical engineering.

CRediT authorship contribution statement

Zeyuan Wang: Writing – review & editing, Writing – original draft, Visualization, Validation, Software, Methodology, Investigation, Formal analysis, Data curation, Conceptualization. **Mohammed Chadli:** Writing – review & editing, Validation, Supervision, Resources, Project administration, Methodology, Funding acquisition, Conceptualization. **Steven X. Ding:** Writing – review & editing, Validation, Resources.

Declaration of competing interest

The authors declare that they have no known competing financial interests or personal relationships that could have appeared to influence the work reported in this paper.

Acknowledgments

The authors would like to express their sincere appreciation to the Editor and the reviewers for their valuable suggestions and comments.

This work was supported by the China Scholarship Council [grant number 202206020096].

Appendix A. Proof of Corollary 6

Proof. Begin with (11), a lower bound of ω_i could be found by using following inequalities:

$$\psi_i \boldsymbol{e}_i^T \boldsymbol{P}_3 \boldsymbol{e}_i \geq \psi_i \eta \|\boldsymbol{e}_i\|^2 \tag{A.1}$$

$$\begin{aligned}\boldsymbol{\Pi}_1 \leq \Big(&-\frac{\epsilon}{2} + k\|\boldsymbol{M}\|^2 + \psi_i\theta_i\|\mathrm{Sym}(\boldsymbol{P}_3\boldsymbol{A})\| + \|\mathrm{Sym}(\boldsymbol{\Psi}\boldsymbol{\mathcal{H}} \otimes \boldsymbol{R}_1^T)\| \\ &+ \frac{1}{b_1}\|\boldsymbol{\Psi}\boldsymbol{\mathcal{H}}\|^2\|\boldsymbol{R}_1\|^2 + \frac{1}{b_2}\psi_i^2\theta_i^2\|\boldsymbol{R}_2\|^2\Big)\boldsymbol{I}_n\end{aligned} \tag{A.2}$$

and

$$\begin{aligned}\boldsymbol{e}_i^T\boldsymbol{\Pi}_3\boldsymbol{z}_i &= -2\psi_i\theta_i\boldsymbol{e}_i^T\boldsymbol{R}_3\boldsymbol{z}_i \\ &\leq \psi_i\left(\frac{1}{\sigma}\theta_i^2\|\boldsymbol{R}_3\|^2\boldsymbol{e}_i^T\boldsymbol{e}_i + \sigma\boldsymbol{z}_i^T\boldsymbol{z}_i\right)\end{aligned} \tag{A.3}$$

Substituting (A.1), (A.2) and (A.3) into (11) and using the relation that $\frac{\epsilon\bar{\delta}_{\min}}{2} - \frac{1}{k} - \psi_i\sigma = 0$, one can obtain

$$\begin{aligned}\omega_i &\geq -\frac{-\epsilon/2 + k\|\boldsymbol{M}\|^2 + \beta + \gamma\|\boldsymbol{R}_1\|^2/b_1}{\psi_i\eta} - \frac{\alpha}{\eta}\theta_i - \frac{1}{\eta}\left(\frac{\psi_i\|\boldsymbol{R}_2\|^2}{b_2} + \frac{\|\boldsymbol{R}_3\|^2}{\sigma}\right)\theta_i^2 \\ &= -(c_0 + c_1\theta_i + c_2\theta_i^2)\end{aligned} \tag{A.4}$$

Then one can conclude that the time required for θ_i decreasing from $\bar{\theta}_i$ to 0 is lower bounded by

$$t_{\min}^i = \int_{\bar{\theta}_i}^0 \frac{1}{\min(-(c_0 + c_1 h + c_2 h^2), 0) - \tau_i}\mathrm{d}h \tag{A.5}$$

which is equivalent to (26).

Appendix B. Proof of Corollary 7

Proof. Using the change of variable of $\boldsymbol{F} = \boldsymbol{P}_2\boldsymbol{L}_o$, the term $\boldsymbol{S}_{22}$ in $\boldsymbol{S}$ (9) becomes $\boldsymbol{\Omega}_{22}$. Notice that the matrix $\boldsymbol{S}$ in Theorem 5 could be decomposed into $\boldsymbol{S} = \boldsymbol{\Gamma}^T\boldsymbol{\Lambda}\boldsymbol{\Gamma}$ with $\boldsymbol{\Gamma}$ and $\boldsymbol{\Lambda}$ defined as

$$\boldsymbol{\Gamma} = \begin{pmatrix} \boldsymbol{I}_{Nn} & \boldsymbol{0}_{Nn} \\ \boldsymbol{0}_{Nn} & \boldsymbol{I}_{Nn} \\ \boldsymbol{0}_{Nm\times Nn} & -\boldsymbol{I}_N \otimes \boldsymbol{K} \end{pmatrix} \tag{B.1}$$

$$\boldsymbol{\Lambda} = \begin{pmatrix} \boldsymbol{\Lambda}_{11} & \boldsymbol{0}_{Nn} & \boldsymbol{\Psi}\boldsymbol{\mathcal{H}} \otimes \boldsymbol{P}_1\boldsymbol{B} \\ * & \boldsymbol{\Omega}_{22} & -\boldsymbol{I}_N \otimes \boldsymbol{K}^T \\ * & * & -2\boldsymbol{I}_{Nn} \end{pmatrix} \tag{B.2}$$

where $\boldsymbol{\Lambda}_{11} = \boldsymbol{\Psi} \otimes (\mathrm{Sym}(\boldsymbol{P}_1\boldsymbol{A})) - \mathrm{Sym}((\boldsymbol{\Psi}\boldsymbol{\mathcal{H}}) \otimes (\boldsymbol{P}_1\boldsymbol{B}\boldsymbol{K}))$. Then, $\boldsymbol{\Lambda} < 0$ becomes a sufficient condition for $\boldsymbol{S} < 0$. To find a $\mathcal{LMI}$ form, the idea is to separate $\boldsymbol{P}_1$ and $\boldsymbol{K}$ in $\boldsymbol{\Lambda}_{11}$. One can use the following inequalities:

$$\begin{aligned}&-\mathrm{Sym}((\boldsymbol{\Psi}\boldsymbol{\mathcal{H}}) \otimes (\boldsymbol{P}_1\boldsymbol{B}\boldsymbol{K})) \\ &\leq -\mathrm{Sym}((\boldsymbol{\Psi}\boldsymbol{\mathcal{H}}) \otimes (\boldsymbol{P}_1\boldsymbol{B}\boldsymbol{K})) + \mu_1^2\boldsymbol{\mathcal{H}}^2 \otimes (\boldsymbol{K}^T\boldsymbol{B}^T\boldsymbol{B}\boldsymbol{K}) \\ &= \left(\frac{\boldsymbol{I}_N \otimes \boldsymbol{P}_1}{\mu_1} - \mu_1\boldsymbol{\Psi}\boldsymbol{\mathcal{H}} \otimes \boldsymbol{B}\boldsymbol{K}\right)^T\left(\frac{\boldsymbol{I}_N \otimes \boldsymbol{P}_1}{\mu_1} - \mu_1\boldsymbol{\Psi}\boldsymbol{\mathcal{H}} \otimes \boldsymbol{B}\boldsymbol{K}\right) - \frac{\boldsymbol{I}_N \otimes \boldsymbol{P}_1^2}{\mu_1^2}\end{aligned} \tag{B.3}$$

with $\mu_1 > 0$, and

$$-\frac{\boldsymbol{I}_N \otimes \boldsymbol{P}_1^2}{\mu_1^2} \leq \boldsymbol{I}_{Nn} - 2\frac{\boldsymbol{I}_N \otimes \boldsymbol{P}_1}{\mu_1} \tag{B.4}$$

Then it follows that

$$\begin{aligned}&-\mathrm{Sym}((\boldsymbol{\Psi}\boldsymbol{\mathcal{H}}) \otimes (\boldsymbol{P}_1\boldsymbol{B}\boldsymbol{K})) \\ &\leq \left(\frac{\boldsymbol{I}_N \otimes \boldsymbol{P}_1}{\mu_1} - \mu_1\boldsymbol{\Psi}\boldsymbol{\mathcal{H}} \otimes \boldsymbol{B}\boldsymbol{K}\right)^T\left(\frac{\boldsymbol{I}_N \otimes \boldsymbol{P}_1}{\mu_1} - \mu_1\boldsymbol{\Psi}\boldsymbol{\mathcal{H}} \otimes \boldsymbol{B}\boldsymbol{K}\right) + \boldsymbol{I}_{Nn} - 2\frac{\boldsymbol{I}_N \otimes \boldsymbol{P}_1}{\mu_1}\end{aligned} \tag{B.5}$$

Therefore by replacing $\boldsymbol{\Lambda}_{11}$ by (B.5) in $\boldsymbol{\Lambda}$ (B.2) and the Schur complement, one can obtain the matrix $\boldsymbol{\Omega}$ in (30).

Appendix C. Proof of Corollary 9

Proof. One can first perform a change of variable of $\boldsymbol{F} = \boldsymbol{P}_2\boldsymbol{L}_o$ thus the term $\boldsymbol{S}_{22}$ in $\boldsymbol{S}$ (9) becomes $\boldsymbol{\Xi}_{22}$. Based on Assumption 8 that $\boldsymbol{B}$ has full column rank, inspired by [41], $(\boldsymbol{B}^T\boldsymbol{B})$ is invertible, then it follows from the linear matrix equality $\boldsymbol{BR} = \boldsymbol{P}_1\boldsymbol{B}$ that $\boldsymbol{R}$ is also full rank, thus $\boldsymbol{R} = (\boldsymbol{B}^T\boldsymbol{B})^{-1}\boldsymbol{B}^T\boldsymbol{P}_1\boldsymbol{B}$ and $\boldsymbol{R}$ is invertible which yields $\boldsymbol{B} = \boldsymbol{P}_1\boldsymbol{B}\boldsymbol{R}^{-1}$. Using the change of variable $\boldsymbol{N} = \boldsymbol{RK}$, we have

$$(\boldsymbol{\Psi}\boldsymbol{\mathcal{H}}) \otimes (\boldsymbol{P}_1\boldsymbol{BK}) = (\boldsymbol{\Psi}\boldsymbol{\mathcal{H}}) \otimes (\boldsymbol{BRK}) = (\boldsymbol{\Psi}\boldsymbol{\mathcal{H}}) \otimes (\boldsymbol{BN}) \tag{C.1}$$

Replace $\boldsymbol{S}_{11}$ and $\boldsymbol{S}_{12}$ in (9) with (C.1) yields:

$$\begin{aligned}\boldsymbol{S}_{11} &= \boldsymbol{\Psi} \otimes \mathrm{Sym}(\boldsymbol{P}_1\boldsymbol{A}) - \mathrm{Sym}((\boldsymbol{\Psi}\boldsymbol{\mathcal{H}}) \otimes (\boldsymbol{P}_1\boldsymbol{BK})) \\ &= \boldsymbol{\Psi} \otimes \mathrm{Sym}(\boldsymbol{P}_1\boldsymbol{A}) - \mathrm{Sym}((\boldsymbol{\Psi}\boldsymbol{\mathcal{H}}) \otimes (\boldsymbol{BN})) = \boldsymbol{\Xi}_{11} \\ \boldsymbol{S}_{12} &= -(\boldsymbol{\Psi}\boldsymbol{\mathcal{H}}) \otimes (\boldsymbol{P}_1\boldsymbol{BK}) = (\boldsymbol{\Psi}\boldsymbol{\mathcal{H}}) \otimes (\boldsymbol{BN}) = \boldsymbol{\Xi}_{12}\end{aligned} \tag{C.2}$$

Therefore $\boldsymbol{\Xi} < 0$ is a sufficient condition for $\boldsymbol{S} < 0$ in (8), which completes the proof.

Data availability

Data will be made available on request.

References

[1] Wei Ni, Daizhan Cheng, Leader-following consensus of multi-agent systems under fixed and switching topologies, Systems Control Lett. 59 (3–4) (2010) 209–217.

[2] Chuiliu Kong, Ying Wang, Yanlong Zhao, Asymptotic consensus of multi-agent systems under binary-valued observations and observation uncertainty, Systems Control Lett. 182 (2023) 105656.

[3] Kai Zhang, Bin Zhou, Guang-Ren Duan, Leader-following consensus of multi-agent systems with time delays by fully distributed protocols, Systems Control Lett. 178 (2023) 105582.

[4] Zeyuan Wang, Mohammed Chadli, Observer-based distributed dynamic event-triggered control of multi-agent systems with adjustable interevent time, Asian J. Control (2024) page asjc.3385.

[5] Xiwang Dong, Bocheng Yu, Zongying Shi, Yisheng Zhong, Time-varying formation control for unmanned aerial vehicles: Theories and applications, IEEE Trans. Control Syst. Technol. 23 (1) (2015) 340–348.

[6] Kwang-Kyo Oh, Myoung-Chul Park, Hyo-Sung Ahn, A survey of multi-agent formation control, Automatica 53 (2015) 424–440.

[7] Aibing Qiu, Ahmad W. Al-Dabbagh, Tongwen Chen, A tradeoff approach for optimal event-triggered fault detection, IEEE Trans. Ind. Electron. 66 (3) (2019) 2111–2121.

[8] Xian-Ming Zhang, Qing-Long Han, Xiaohua Ge, Derui Ding, Lei Ding, Dong Yue, Chen Peng, Networked control systems: a survey of trends and techniques, IEEE/CAA J. Autom. Sin. 7 (1) (2020) 1–17.

[9] Paulo Tabuada, Event-triggered real-time scheduling of stabilizing control tasks, IEEE Trans. Autom. Control 52 (2007) 1680–1685.

[10] Dimos V. Dimarogonas, Emilio Frazzoli, Karl H. Johansson, Distributed event-triggered control for multi-agent systems, IEEE Trans. Autom. Control 57 (5) (2012) 1291–1297.

[11] Zeyuan Wang, Mohammed Chadli, Distributed observer-based dynamic event-triggered control of multi-agent systems with adjustable inter-event time, in: 2023 62nd IEEE Conference on Decision and Control, CDC, IEEE, Singapore, Singapore, 2023, pp. 2391–2396.

[12] Yanan Qi, Xianfu Zhang, Rui Mu, Yanjie Chang, Bipartite consensus for high-order nonlinear multi-agent systems via event-triggered/self-triggered control, Systems Control Lett. 172 (2023) 105439.

[13] Congcong Tian, Kaixin Tian, Jie Mei, Guangfu Ma, Bipartite leaderless position consensus of heterogeneous uncertain multi-agent systems under switching directed graphs, Systems Control Lett. 181 (2023) 105628.

[14] Thiem V. Pham, Quynh T. Thanh Nguyen, Adaptive formation control of nonlinear multi-agent systems with dynamic event-triggered communication, Systems Control Lett. 181 (2023) 105652.

[15] Xiaohua Ge, Qing-Long Han, Distributed formation control of networked multi-agent systems using a dynamic event-triggered communication mechanism, IEEE Trans. Ind. Electron. 64 (10) (2017) 8118–8127.

[16] Cameron Nowzari, Eloy Garcia, Jorge Cortés, Event-triggered communication and control of networked systems for multi-agent consensus, Automatica 105 (2019) 1–27.

[17] Antoine Girard, Dynamic triggering mechanisms for event-triggered control, IEEE Trans. Autom. Control 60 (7) (2015) 1992–1997.

[18] Xiaohua Ge, Qing-Long Han, Xian-Ming Zhang, Derui Ding, Dynamic event-triggered control and estimation: A survey, Int. J. Autom. Comput. 18 (6) (2021) 857–886.

[19] Xin Meng, Baoping Jiang, HamidReza. Karimi, Cunchen Gao, Leader–follower sliding mode formation control of fractional-order multi-agent systems: A dynamic event-triggered mechanism, Neurocomputing 557 (2023) 126691.

[20] Yanping Yang, Bo Shen, Qing-Long Han, Dynamic event-triggered scaled consensus of multi-agent systems in reliable and unreliable networks, IEEE Trans. Syst. Man Cybern. Syst. (2023) 1–13.

[21] Zeyuan Wang, Mohammed Chadli, Improved dynamic event-triggered consensus control for multi-agent systems with designable inter-event time*, in: 2023 31st Mediterranean Conference on Control and Automation, MED, IEEE, Limassol, Cyprus, 2023, pp. 818–823.

[22] Qinghua Hou, Jiuxiang Dong, Robust adaptive event-triggered fault-tolerant consensus control of multiagent systems with a positive minimum interevent time, IEEE Trans. Syst. Man Cybern. Syst. 53 (7) (2023) 4003–4014.

[23] Jiantao Shi, Cooperative control for nonlinear multi-agent systems based on event-triggered scheme, IEEE Trans. Circuits Syst. II 68 (6) (2021) 1977–1981.

[24] Zheng-Guang Wu, Yong Xu, Renquan Lu, Yuanqing Wu, Tingwen Huang, Event-triggered control for consensus of multiagent systems with fixed/switching topologies, IEEE Trans. Syst. Man Cybern. Syst. 48 (10) (2018) 1736–1746.

[25] James Berneburg, Cameron Nowzari, Distributed dynamic event-triggered coordination with a designable minimum inter-event time, in: 2019 American Control Conference, ACC, 2019, pp. 1424–1429.

[26] Xiaoqun Wu, Bing Mao, Xiuqi Wu, Jinhu Lu, Dynamic event-triggered leader-follower consensus control for multiagent systems, SIAM J. Control Optim. 60 (1) (2022) 189–209.

[27] Xing Chu, Na Huang, Zhiyong Sun, Event triggering control for dynamical systems with designable inter-event times, IFAC-PapersOnLine 53 (2) (2020) 6410–6415.

[28] Kai Zhang, Bin Zhou, Xuefei Yang, Guang-Ren Duan, Time-varying event-triggered and self-triggered bounded control of linear systems with a designable minimal interevent time, IEEE Trans. Syst. Man Cybern. Syst. (2023).

[29] Meilin Li, Yue Long, Tieshan Li, Hongjing Liang, C.L. Philip Chen, Dynamic event-triggered consensus control for input constrained multi-agent systems with a designable minimum inter-event time, IEEE/CAA J. Autom. Sin. 10 (2023) 1–12.

[30] Hao Zhang, Gang Feng, Huaicheng Yan, Qijun Chen, Observer-based output feedback event-triggered control for consensus of multi-agent systems, IEEE Trans. Ind. Electron. 61 (9) (2014) 4885–4894.

[31] Jiangping Hu, Ji Geng, Hong Zhu, An observer-based consensus tracking control and application to event-triggered tracking, Commun. Nonlinear Sci. Numer. Simul. 20 (2) (2015) 559–570.

[32] Guoliang Zhu, Kexin Liu, Haibo Gu, Weilin Luo, Jinhu Lü, Observer-based event-triggered formation control of multi-agent systems with switching directed topologies, IEEE Trans. Circuits Syst. I. Regul. Pap. 69 (3) (2022) 1323–1332.

[33] Juan Antonio Vazquez Trejo, Mohammed Chadli, Damiano Rotondo, Manuel Adam Medina, Didier Theilliol, Event-triggered fault-tolerant leader-following control for homogeneous multi-agent systems, IFAC-PapersOnLine 55 (6) (2022) 79–84.

[34] Xiaoli Ruan, Jianwen Feng, Chen Xu, Jingyi Wang, Observer-based dynamic event-triggered strategies for leader-following consensus of multi-agent systems with disturbances, IEEE Trans. Netw. Sci. Eng. 7 (4) (2020) 3148–3158.

[35] Ijaz Ahmed, Muhammad Rehan, Naeem Iqbal, ChoonKi Ahn, A novel event-triggered consensus approach for generic linear multi-agents under heterogeneous sector-restricted input nonlinearities, IEEE Trans. Netw. Sci. Eng. (2023) 1–10.

[36] Mengyang Xu, Mingxing Li, Fei Hao, Fully distributed optimization of second-order systems with disturbances based on event-triggered control, Asian J. Control (2023) 1–14.

[37] Eloy Garcia, Yongcan Cao, David Wellman Casbeer, Decentralized event-triggered consensus with general linear dynamics, Automatica 50 (10) (2014) 2633–2640.

[38] Changbin (Brad) Yu, Jiahu Qin, Huijun Gao, Cluster synchronization in directed networks of partial-state coupled linear systems under pinning control, Automatica 50 (9) (2014) 2341–2349.

[39] Yong Xu, Mei Fang, Zheng-Guang. Wu, Ya-Jun Pan, Mohammed Chadli, Tingwen Huang, Input-based event-triggering consensus of multiagent systems under denial-of-service attacks, IEEE Trans. Syst. Man Cybern. Syst. 50 (4) (2020) 1455–1464.

[40] Yong Xu, Mei Fang, Peng Shi, Zheng-Guang Wu, Event-based secure consensus of mutiagent systems against dos attacks, IEEE Trans. Cybern. 50 (8) (2020) 3468–3476.

[41] C.A.R. Crusius, A. Trofino, Sufficient lmi conditions for output feedback control problems, IEEE Trans. Autom. Control 44 (5) (1999) 1053–1057.